THE JOURNAL OF COMPARATIVE NEUROLOGY 385:95–116 (1997)

The Timetable of Laminar Neurogenesis Contributes to the Specification of Cortical Areas in Mouse Isocortex

FRANCK POLLEUX, COLETTE DEHAY, AND HENRY KENNEDY*
INSERM U371-Cerveau et Vision, 69675 Bron Cedex, France

ABSTRACT

In the primate visual cortex, the birthdate of neurons in homologous layers differ on either side of the 17-18 border suggesting that there might be different timetables of laminar histogenesis in these two areas (Dehay et al. [1993] Nature *366:*464–466 and Kennedy et al. [1996] Soc. Neurosci. Abst. *22:*525). Because of the potential importance of these findings for understanding mechanisms that generate areal identity, we have developed an experimental approach that makes it possible to accurately compute the timetable of laminar histogenesis from birthdating experiments. Here we report the results of an exhaustive examination of the tempo of layer production in five cortical areas of the mouse. Tritiated thymidine pulse injections were made during embryonic development and labeled neurons were examined in three frontoparietal areas (areas 3, 4, and 6) and two occipital areas (areas 17 and 18a) of the adult cortex. The correlation between the radial distribution of neurons and the intensities of labeling enabled us to reliably identify first generation neurons (i.e., those neurons that quit the cell-cycle in the first round of mitosis after injection). For each cortical layer, the percentage of first generation neurons with respect to the total number of neurons defined a laminar labeling index. Changes of the laminar labeling index over time determined the timetable of layer formation. The onset and duration of layer formation was identical in the two occipital areas. This finding contrasted with the frontoparietal areas where there were important differences in the timing of infragranular and granular layer formation and noticeably production of layers VIa, V, and IV occurs earlier in area 3 than in area 6. The timing of laminar production of areas 17 and 18a resembles more that of area 3 than that of area 6. With respect to areas 3 and 6, area 4 shows an intermediate but significantly different timetable of layer production. These marked areal differences in the timetable of laminar histogenesis contrasted with the relative homogeneity within areas so that we have been able to demonstrate that the interareal differences are not merely the expression of known neurogenic gradients.

These results suggest that in the mouse frontoparietal isocortex, neighbouring regions of the ventricular zone that will give rise to distinct areas follow distinct programs of layer production. These areal differences occur before thalamic innervation and suggest an early regionalisation of laminar histogenesis. J. Comp. Neurol. 385:95–116, 1997.

Indexing terms: tritiated thymidine; birthdating; cerebral cortex; regionalisation; cortical development

The isocortex is subdivided into radial domains (layers) and tangential domains (areas). Each cortical area is dedicated to the information processing of an aspect of cognitive, sensory, or motor activity. The cortical layers exhibit stereotyped connectivity and physiology which display a number of common features across areas. Investigations of the mechanisms specifying these two sets of compartments have tended to emphasise the early specification of the cortical layers (Caviness, 1976; McConnell, 1988; Rakic, 1988; McConnell and Kaznowski, 1991; Frantz and McConnell, 1996) and the late specification of cortical areas in response to epigenetic clues (O'Leary, 1989). This has led to the suggestion that there may be important differences between the mechanisms that specify these

Grant sponsor: E.E.C.; Grant number: SCI 622; Grant sponsor: BIOMED; Grant number: PL.951604.

*Correspondence to: Dr. Henry Kennedy, INSERM U371-Cerveau et Vision, 18 avenue du doyen Lépine, 69675 Bron Cedex, France. E-mail: kennedy@lyon151.inserm.fr

Received 1 November 1996; Revised 25 February 1997; Accepted 31 March 1997

two cortical compartments (Shatz, 1992). However, recent results show that early specification may be playing a much stronger role in the development of areas (Dehay et al., 1993; Cohen-Tannoudji et al., 1994; Ebrahimi-Gaillard et al., 1994; Ebrahimi-Gaillard and Roger, 1996), emphasising the need to understand cortical development as a mesh of both early and late specification mechanisms in which environmental influences act on early formed patterns (Rakic, 1988; Kennedy and Dehay, 1993). Here, we report findings showing that there are important areal constraints on the timing of layer formation, suggesting a tight coupling in the developmental mechanisms specifying cortical layers and areas.

It has now been established that neurons which undergo their last round of division early in cortical neurogenesis are destined for infragranular layers, and successive later generated neurons take up progressively more superficial positions (Angevine and Sidman, 1961; Berry and Rogers, 1965; Hicks and D'Amato, 1968; Fernandez and Bravo, 1974; Rakic, 1974; Smart and Smart, 1977; Caviness, 1982; Smart and Smart, 1982; Luskin and Shatz, 1985; Jackson et al., 1989; Sanderson and Weller, 1990; Bayer and Altman, 1991; Dehay et al., 1993). Experiments in *reeler* mutant mice first addressed the relation of a neuron's birthdate to its laminar position. In this autosomal recessive mutant, migration of immature cortical neurons is perturbed and neurons cannot bypass earlier generated neurons (Caviness and Sidman, 1973; Caviness, 1982; Pinto Lord et al., 1982; Hoffart et al., 1995). Cortical neuron phenotype in the mutant suggested that the birthdate of cortical neurons determines their future integration in the cortex (Caviness and Sidman, 1973; Caviness, 1976; Dräger, 1981; Lemmon and Pearlman, 1981; Caviness, 1982; Simmons and Pearlman, 1983; Terashima et al., 1983, 1985; Silva et al., 1991). The role of birthdate in specifying cortical layer has been further explored in studies of heterochronic transplantation experiments (McConnell, 1988; McConnell and Kaznowski, 1991; Frantz and McConnell, 1996), layer deletion (Jensen and Altman, 1982; Jensen and Killackey, 1984; Gillies and Price, 1993; Woo and Finlay, 1996), and cell lineage (Price and Thurlow, 1988; Parnavelas et al., 1991; Walsh and Cepko, 1992; Kornack and Rakic, 1995; Reid et al., 1995). These experiments suggest that progenitors are multipotent and that their laminar fate is specified by environmental factors shortly after S phase of the final round of mitosis (McConnell, 1996).

Certain results of birthdating experiments also have been interpreted as evidence in favour of a regionalisation of the commitment to a particular layer of neuroblasts undergoing their final mitosis. Pulse injections of labeled thymidine ([^{3}H]thymidine) lead to a laminar distribution of labeled neurons in the adult that is determined by the age of injection. Injection of [^{3}H]thymidine on a given day led to labeled neurons in the allocortex and hippocampus that differed in their radial height in the rodent (Angevine, 1965) and monkey (Rakic and Nowakowski, 1981). These observations were extended to the monkey visual cortex, where a single pulse of [^{3}H]thymidine gives rise to differences in the laminar distribution of labeled neurons in striate and extrastriate cortex (Rakic, 1976; Dehay et al., 1993). In these experiments, differences in the laminar distribution of labeled neurons on either side of the striate border (Dehay et al., 1993) are potentially significant because they suggest that precursors separated by only a few hundred microns could be generating different layers at any given time.

These speculations concerning the possible areal differences in the specification of cortical layers are based on differences in the laminar distribution of labeled neurons in the mature cortex. However, extensive cell death has been demonstrated in the developing cortex (Blaschke et al., 1996), and Finlay (Finlay and Slattery, 1983) has attributed an important role to differential cell death between the cortical layers in establishing cytoarchitectonic features. It therefore remains an open question whether areal differences in the laminar distribution of [^{3}H]thymidine labeled neurons truly reflect areal differences in the timetable of layer production.

To investigate this issue we have examined the onset and duration of layer formation in adjacent cortical areas in the mouse by using pulse injections of [^{3}H]thymidine. We have developed a quantitative technique that cannot be biased by differential cell death. This was achieved by computing a laminar generation rate from the percentage of labeled neurons in each layer. Because cell death will equally affect the numbers of labeled and unlabeled neurons, this ratio allows an unbiased detection of differences in the onset and duration of layer production. We have chosen neighbouring areas which, like areas 17 and 18 in the monkey, have significant cytoarchitectonic differences, particularly in the numbers of neurons in individual layers (Rockel et al., 1980). These conditions are met by the primary somatosensory area, area 3 and the motor areas 4 and 6 (Beaulieu, 1993; Skoglund et al., 1996). We have measured the timetable of layer production in these three areas and compared them with those in occipital areas 17 and 18a. This reveals important differences in the timing of the major phase of production of layers VIa to IV in areas 3, 4, and 6, whereas the timing of the production of these layers was identical in areas 17 and 18a. We have examined the timetable of laminar histogenesis at separate lateromedial and rostrocaudal positions within individual areas. This shows that the differences between cortical areas are considerably larger than those caused by neurogenic gradients within areas. These results demonstrate an areal regionalisation of layer production in the rodent isocortex and suggest that the coupling of areal and laminar specification might be a general mammalian feature in the development of the isocortex.

MATERIALS AND METHODS

Breeding procedure

Animal care procedures are in accordance with current requirements in France. Eleven timed-pregnant Balb/C mice (IFFA CREDO, Lyon, France) received a single intraperitoneal injection of [methyl-^{3}H]thymidine (Amersham, England; specific activity: 25 Ci/mmol, dose injected: 5 µCi/g of body weight) at different gestational ages (from embryonic day 11.5 [E11.5] to E19.5 see Table 1). Females were put in the presence of males overnight, inspection of mating was carried out the following morning (9:00 A.M.), and when a vaginal plug was found, that day was designated E1. All [^{3}H]thymidine injections were performed between 12:00 and 2:00 PM to overcome problems linked to circadian variations of proliferative activity (Miller, 1992). Two females (litter injected on E14.0 and E16.0) were put with males during a 2-hour period at midday (12:00–2:00 PM) instead of overnight as for the other females. Because

TABLE 1. Summary of the Number of Animals Examined per Litter, the Age in Embryonic Days at Tritiated Thymidine Injection, and the Range of Maximal Number of Silver Grains per Nucleus for Each Litter

Embryonic day (E) of [^{3}H]thymidine injection	Number of animals examined per litter	Range of the maximal number of silver grains per nucleus observed in each litter
E11.5	3	44–46
E12.5	2	78–81
E13.5	3	68–72
E14.0	3	73–76
E14.5	3	78–81
E15.5	2	77–80
E16.0	3	75–78
E16.5	2	63–65
E17.5	3	40–43
E18.5	3	32–34
E19.5	3	3–4

[^{3}H]thymidine injections were carried out at midday, these two litters are designated E14.0 and E16.0, whereas the nine others all fell on the half-day periods (see Table 1). Animals were killed at adulthood by a lethal injection of sodium pentobarbital and perfused transcardially with a saline buffered solution, pH 7.4 (0.9% NaCl in 0.1 M phosphate buffer [PB] with 1 g/liter of Procaine) followed by a solution of 4% paraformaldehyde in the same buffer solution.

Histology and autoradiographic procedure

The brains were removed, postfixed in the same solution for 2 days, rinsed in running tap water overnight, dehydrated by immersion in graded ethanol solutions (70–100%) and cleared in toluene. The brains were embedded in wax, cut serially (10 microns), and mounted on glass slides with a 5% albumin-gelatin mixture. One in six sections were dewaxed, rehydrated, air dried, and dipped in autoradiographic Ilford K2 emulsion (45% in distilled water at 40°C). Sections were stored in a desiccating box for an exposure of 6–8 weeks (4°C), developed with Ilford PQ Universal (10%, 19°C, 5 minutes), and fixed with Ilfospeed (20%, 20°C, 5 minutes). The sections were rinsed, air dried, counterstained with cresyl violet (0.1%, 7–8 minutes), and mounted with Depex. One possible source of error in the estimation of the total number of neurons (T) is incomplete Nissl staining. In the present study, staining procedure and section thickness ensured optimal staining (Cooper et al., 1988).

Acetylcholinesterase (AchE) and NADPH-diaphorase histochemistry

AchE and NADPH-diaphorase activity were used to localise cortical areas in adult Balb/C mice (3–4 months old). The animals were perfused according to the same procedure as described above before being passed through a sucrose gradient (10–30% in PB, 0.1 M, pH = 7.4). The brains were removed and 40-micron-thick coronal sections cut on a freezing microtome. AchE histochemistry was performed according to a protocol by using acetylthiocholine iodide as the substrate (Hardy et al., 1976). Incubation times ranged from 3 to 4 hours at 37°C. NADPH-diaphorase histochemistry was performed on sections adjacent to those reacted for AchE (Vincent and Kimura, 1992).

Quantification of autoradiographic labeling

The autoradiographic signal was analysed by using a light microscope (Dialux 20, Leitz, Bron, France) coupled to an interactive system of plotting (Microvid, Leitz), piloted by Histovid software (BIOCOM™). Five hundred-micron-wide radial strips of cytoarchitectonically identified neocortical areas were examined by using an image projected on a VGA BARCO screen (CD 233) captured by a CCD COHU camera. Care was taken to ensure that the distances between strips in areas 3 and 6 and in areas 17 and 18a had similar separations. The maximal number of silver grains over a single nucleus was estimated for each brain. Grains were counted over nuclear profiles at a final magnification of ×3,140 and corrected for apparent diameter (Appleton et al., 1969). Although the maximal number of silver grains varies between litters (range, 32–81), this number is remarkably constant within a given litter (see Table 1). Background levels are less than 1 silver grain per mean nuclear surface. The distinction between neurons and glia is based on the mean dimensions of the nucleus (neurons, 8–23 microns; glia, 4–6 microns) and the absence of visible glial cytoplasm with cresyl violet stain (see Fig. 1). Two additional morphological criteria are the clumps of chromatin along the nuclear membrane of glia as well as the frequent presence of a nucleolus in the neuronal nucleus (Heumann and Leuba, 1983).

Neurons showing heavy labeling (and which were identified as first generation [FG] neurons, >50% of maximum labeling) were plotted in each layer of all five areas. Proportions of FG neurons in each layer were estimated with respect to the total number (T) of [^{3}H]thymidine labeled and unlabeled neurons. Because FG and T populations are from the same layer and have the same shape and size, cell counts did not have to be corrected for splitting errors. The data points for each age were compiled from six sections corresponding to two or three nonadjacent sections in two or three animals taken from one litter. The distance of the labeled nucleus from the white-matter/grey-matter limit was expressed as a percentage value of the cortical height and used to quantify the radial distribution of different categories of labeled neurons (Terashima et al., 1985).

Statistical analysis

The autoradiographic labeling intensity of approximately 150,000 neurons was quantitatively examined for the study of areas 6, 4, and 3 and approximately 130,000 neurons for the study of areas 17 and 18a. Statistical analysis (χ^2) was performed by using Statview 4.02 software (Deltasoft, Meyland, France). At each age, variability of values in a given area (intragroup comparisons) was tested and failed to show any statistical significance. Intergroup comparisons were then performed to reveal [FG/T] variations between homologous layers in separate areas.

RESULTS

Autoradiographic labeling is illustrated in a high power view in Figure 1 taken from parietal cortex after injection on E14.5. Individual silver grains can be distinguished, allowing numbers of grains per nuclei to be used to estimate the labeling density of individual neurons. This made it possible to allocate labeled neurons to different categories. The background level has been estimated by calculating the density of silver grains in extracellular space (Rogers, 1967) and in all cases was inferior to 1 grain

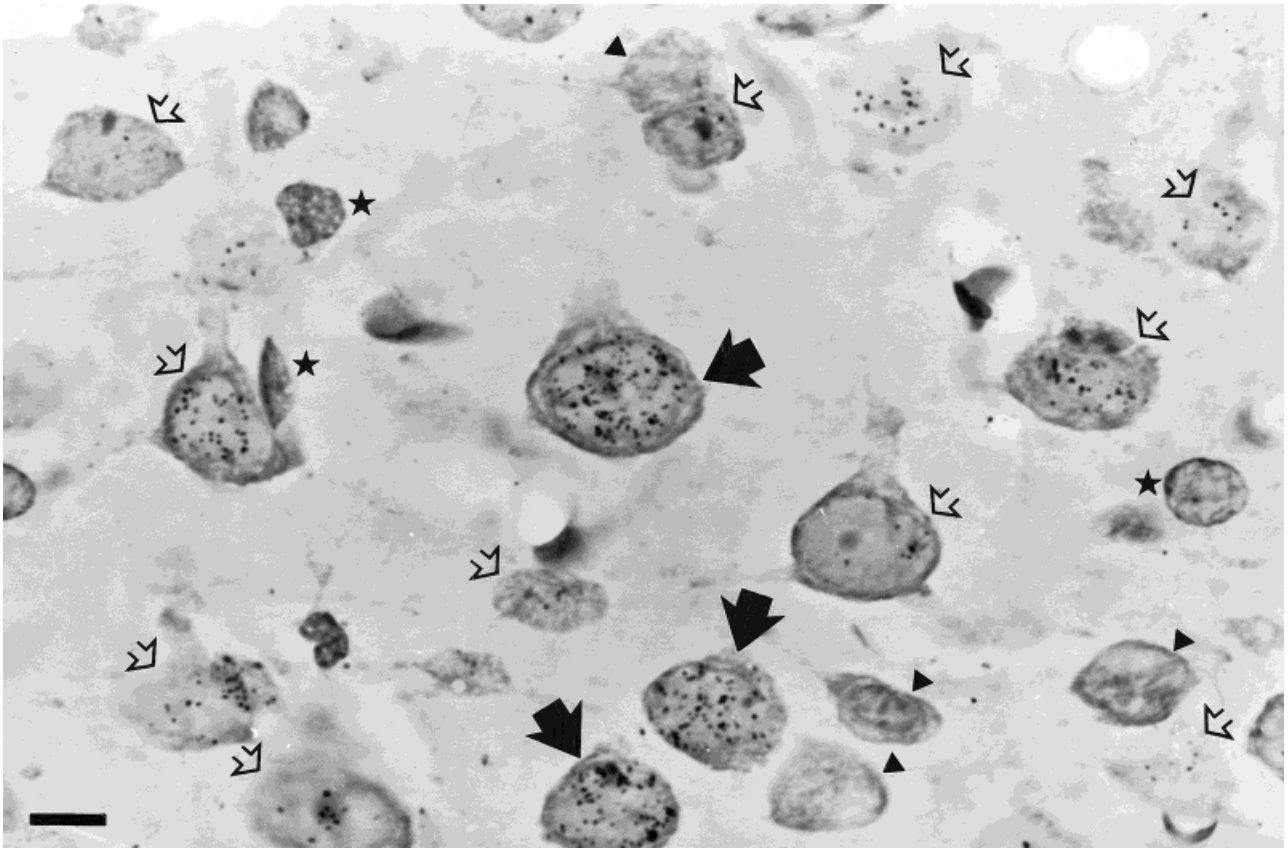

Fig. 1. Autoradiographic signal of layer V neurons in area 3 after an E14.5 [^{3}H]thymidine injection. Silver grain counts allow estimation of different categories of labeling. First generation (FG) neurons are indicated by large arrows, subsequently generated (SG) neurons by open arrows, and unlabeled neurons by arrowheads. Asterisks indicate glial cells. Note the low level of autoradiographic background. Scale bar = 10 microns.

per 400 mm^2 (i.e., much lower than 1 silver grain per nuclear profile).

Identification of cortical areas

The distribution of labeled neurons was examined at adulthood, thereby allowing us to relate developmental changes to areal and laminar boundaries on the basis of cytoarchitectonic criteria (Fig. 2) (Krieg, 1946a,b; Woolsey and van der Loos, 1970; Caviness, 1975). Area 3, the primary somatosensory area, exhibits a well developed layer IV and nearly 27% (Beaulieu, 1993) to 43% (Skoglund et al., 1996) more neurons under a unit area of cortical surface than does the primary motor area, area 6, which has a much thinner layer IV (Caviness, 1975; Skoglund et al., 1997). These two areas are separated by a narrow band of area 4, which exhibits intermediate cytoarchitectonic features (Caviness, 1975) as shown in Figure 2C. Areas 17 and 18a can also be distinguished on cytoarchitectonic grounds. Compared with area 18a, layer IV in area 17 is wider (Krieg, 1946a,b; Caviness, 1975) and has a higher cell density (Finlay and Slattery, 1983).

Although the cortical areas examined in this study can be readily identified in 40-micron-thick sections, they are not apparent in 10-micron sections that are required for the autoradiographic technique. In the present study, we used brains cut on a freezing microtome (40 microns) and processed for histochemistry (NADPH diaphorase and AchE) as an aid to localise cortical areas of interest in the paraffin sections. NADPH diaphorase activity is high in layer IV of areas 3, 4, and 6 (Fig. 2B). In area 3, NADPH diaphorase labels the barrels, and this histochemistry gives a good location of the area 3/4 boundary. In contrast to a previous report (Mitrovic and Schachner, 1996), we find that NADPH is expressed in the adult mouse barrel field. AChE histochemistry was found to label area 17 where activity in layer IV makes it possible to locate the 17/18a boundary (Fig. 2D). This finding corresponds to a species difference, because AchE labeling in area 17 of the rat is restricted to the immature cortex (Robertson et al., 1985; Robertson et al., 1988).

In a second step, all the Nissl stained neurons in each 10-micron-thick section selected for analysis, were plotted at high power magnification (see Materials and Methods). These total cell plots illustrated in Figure 2C,E provide a high definition of the cytoarchitectonic boundaries that are comparable to those obtained in 40-micron-thick sections. Using the total cell plots it is possible to detect the fine cytoarchitectonic details that are detectable in the 40-micron-thick sections and that cannot be observed by mere microscopic inspection of the 10-micron-thick sections. Therefore, in all cases, total cell plots were used to obtain a positive high precision identification of areal and laminar boundaries (Krieg, 1946a,b; Woolsey and van der Loos, 1970; Caviness, 1975).

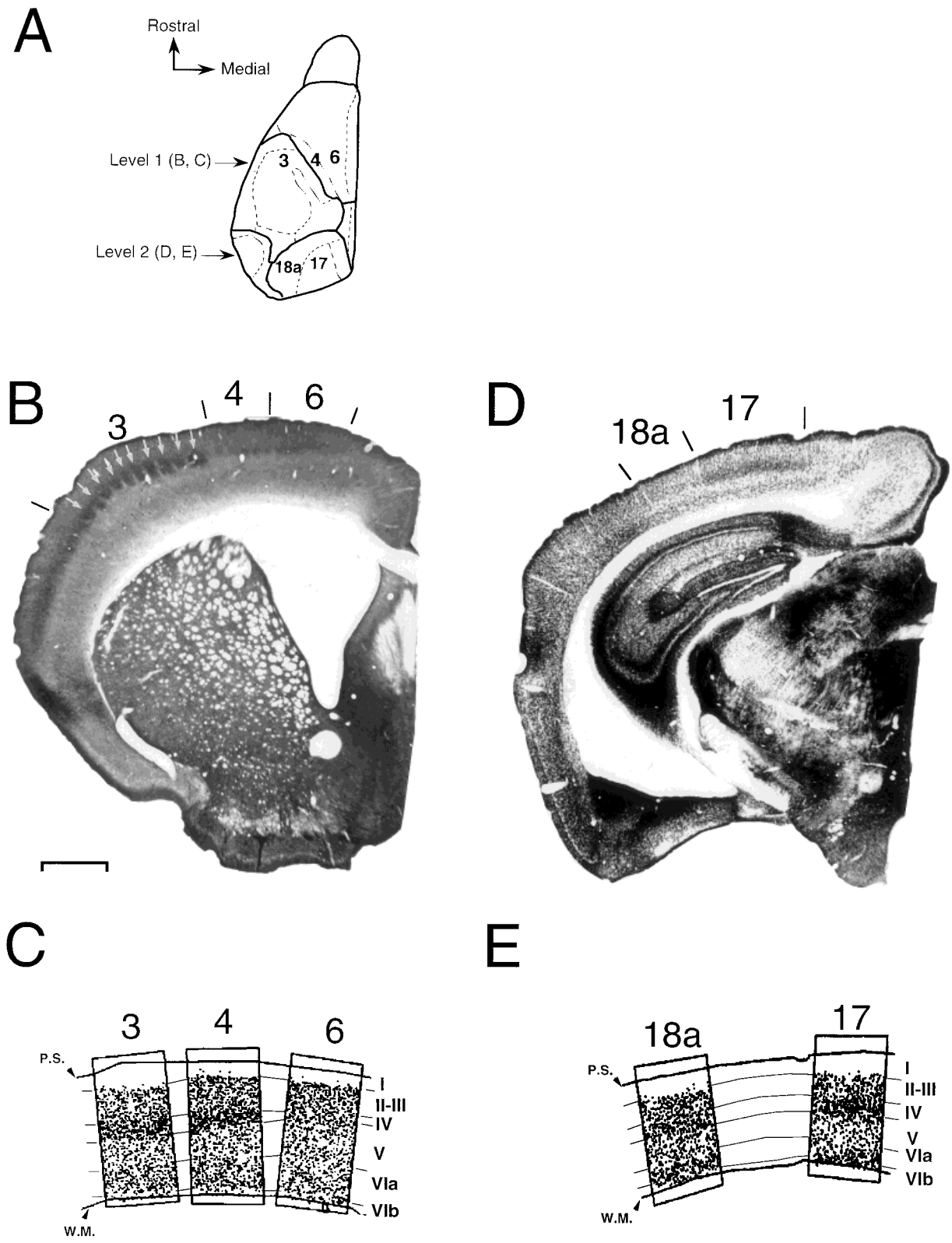

Fig. 2. Cytoarchitectonic and histochemical criteria used to locate the cortical areas examined in the present study. **A:** Architectonic map of mouse neocortex (dorsal view, modified from Caviness, 1975). The anterior-posterior levels examined are indicated by arrows. Full lines indicate the limit between architectonic fields (frontal, parietal, occipital, temporal, and retrosplenial) whereas dashed lines indicate limits between cortical areas. **B:** Photomicrograph of a NADPH diaphorase reacted section taken at Level 1 shown in A. High NADPH diaphorase activity defines layer IV in both frontal and parietal areas. In area 3, individual barrels are clearly observable and are indicated by small arrows. **C:** Plot of all the neurons encountered in 500-micron-wide strips of areas 3, 4, and 6 on a 10-micron-thick paraffin section counterstained with cresyl violet. This plot reveals the pronounced reduction in both cell packing density and thickness of layer IV going from parietal area 3 to frontal area 6. **D:** Photomicrograph of an acetylcholinesterase reacted section taken at Level 2 shown in A. The extent of area 17 is revealed by using this histochemical approach. **E:** Plot of all the neurons encountered in 500-micron-wide strips of areas 17 and 18a on a 10-micron-thick paraffin section counterstained with cresyl violet. This plot shows that occipital area 17 has a more densely packed layer IV than does area 18a. Abbreviations: P.S., pial surface; W.M., white matter/grey matter boundary.

Relationship between intensity of autoradiographic labeling and order of generation

Pulse injections of [^{3}H]thymidine at successive embryonic ages show a staggered distribution of heavily labeled neurons going from layers VIb to II (see Figs. 4–7) as reported by others (Angevine and Sidman, 1961; Smart and Smart, 1977, 1982; Caviness, 1982). In the rodent, the number of successive cell divisions during the period of neuron production has been calculated to be of the order of 11 (Caviness et al., 1995) so that each generation can be expected to occupy successively more superficial radial positions (Smart and Smart, 1977, 1982).

The radial displacement of successive generations can be used as a means of determining the labeling criteria that distinguish first generation neurons from the progeny of the precursors that remain in the cell-cycle and that undergo further division. Figure 3A shows autoradiographic labeling after an injection at E14 during the major phase of layer VIa and VIb production. In this figure, each panel shows the distribution of labeled neurons with a narrow range of labeling intensity. This injection returned a maximum of 76 grains per cell (Table 1). Neurons with maximum labeling (>56 grains, panel 1) are restricted to lower layers. Less densely labeled categories up to and including 41–45 grains (panels 2–4) continue to show a laminar distribution restricted to layers VIa and VIb. Neurons presenting less than 40 grains show a significant increase in the width of their radial distribution. Hence in the 36–41 class (panel 5) labeled neurons spread into layer V. As labeling drops to 16–20 grains per nuclei (panels 6–9) there is a steady increase in the number of labeled neurons in layer V. In the 11–15 class (panel 10) labeled neurons spread into layer IV and in the two lightest categories (panels 11 and 12) labeled neurons are found in the most superficial layers.

To quantify these radial changes we have undertaken a box plot analysis, which permits the comparison of the radial height of different categories of labeled neurons over six nonadjacent sections. In the example shown in Figure 3B, the boxes 1 to 12 on the horizontal axis correspond to the panels 1–12 in Figure 3A. This analysis shows changes of the median heights of labeled neurons in the cortex expressed as a percentage of the radial thickness of the cortex. As labeling intensity drops, the radial dispersion increases and median height is displaced from layer VIb to the top half of layer V. The increase of median height as a percentage of cortical thickness is not monotonic and four inflections can be detected. Boxes 1–4 show median heights ranging from 2–9%; boxes 5–9, 17–21%; boxes 10–12, 34–55%. The first inflection between groups 4 and 5 occurs at the level of 41 grains. This inflection separates labeled neurons into two groups: groups 1–4 containing >50% maximal labeling, which corresponds to FG neurons; and groups 5–12 containing <50% maximal labeling, which corresponds to subsequently generated (SG) neurons. Despite that a contingent of FG neurons will display light levels of labeling (see Discussion), the present results show a clear radial separation between FG and SG neurons. A nonparametric Kolmogorov-Smirnov test was used to compare each pair of distributions (group 1 vs. group 2, 2 vs. 3, etc.) and confirms the statistical significance of the relationship between labeling intensity and the radial distribution of cortical neurons. Significant differences ($P < 0.05$) were only found between groups 4 and 5, 9 and 10, 10 and 11, 11 and 12.

To conclude, this analysis shows that 50% of the maximal labeling can be used as a threshold value to identify FG neurons (i.e., those neurons that left the ventricular zone immediately after the pulse of [^{3}H]thymidine).

Laminar distribution of FG neurons

The laminar location of FG neurons from injections at different embryonic ages reveals the inside-first, outside-last sequence of histogenesis in all five cortical areas. Analysis of the spatial distribution of FG neurons at closely spaced intervals reveals four stages in the neurogenesis of areas 3, 4, and 6 (Fig. 4) and areas 17 and 18a (Fig. 5).

During the first phase (E12.5 in areas 3, 4, and 6 and E12.5–E13.5 in areas 17 and 18a) FG neurons are few and restricted to layers VIa and VIb. During the second phase (E13.5 to E14.5 in areas 3, 4, and 6; E14–E14.5 in areas 17 and 18a), there is an increase in the numbers of FG neurons, and they are located more superficially in the infragranular layers. The third phase (E15.5 to E16.5 all areas) is characterised by peak levels of neuron production and the formation of layer IV. During the fourth and final phase (E17.5 to E18.5 all areas) there is a drop in the number of FG neurons accompanied by an abrupt switch to production of supragranular layers.

Comparison of laminar distributions of FG neurons in areas 3, 4, and 6 suggests there might be important differences in the timing of individual layer formation (Fig. 4). To overcome problems of variation of labeling on individual sections and so as to obtain a clearer representation of the differences in the laminar location of the FG neurons in areas 3, 4, and 6, we prepared charts of cumulative labeling from four neighbouring sections at each age. This permits the identification of clear areal differences in the laminar distribution of labeled neurons at each embryonic stage (Fig. 6). After injection at E12.5, labeling in layers VIa and VIb appears similar in all three areas. After injection at E14.5, there are appreciable numbers of labeled neurons in layer V in area 3, whereas there are few labeled neurons in this layer in area 4 and none in area 6. After injection at E15.5, labeled neurons are present in layer IV in areas 3 and 4, whereas this layer contains no labeled neurons in area 6. After injection at E16, no labeled neurons are present in layer VIa in area 3, whereas this layer contains numerous labeled neurons in areas 6 and 4. There are no obvious differences in the laminar distribution of labeled neurons in areas 3, 4, and 6 at E17.5.

These areal differences in the laminar distribution of labeling in areas 3, 4, and 6 contrast with the similarity in the patterns of labeling in the two occipital areas, areas 17 and 18a (Fig. 7).

Quantitative areal comparison of birthdate of neurons in separate layers

The cumulative plots shown in Figures 6 and 7 provide a visual illustration of the variability of labeling and reveal a radially restricted distribution of FG neurons. The areal differences in the laminar distribution of FG neurons revealed by the cumulative plots suggest that neurons in homologous layers of different areas can be generated at different embryonic ages. To obtain a statistical comparison of areal differences in the laminar distribution we have prepared a series of histograms showing the distribution of

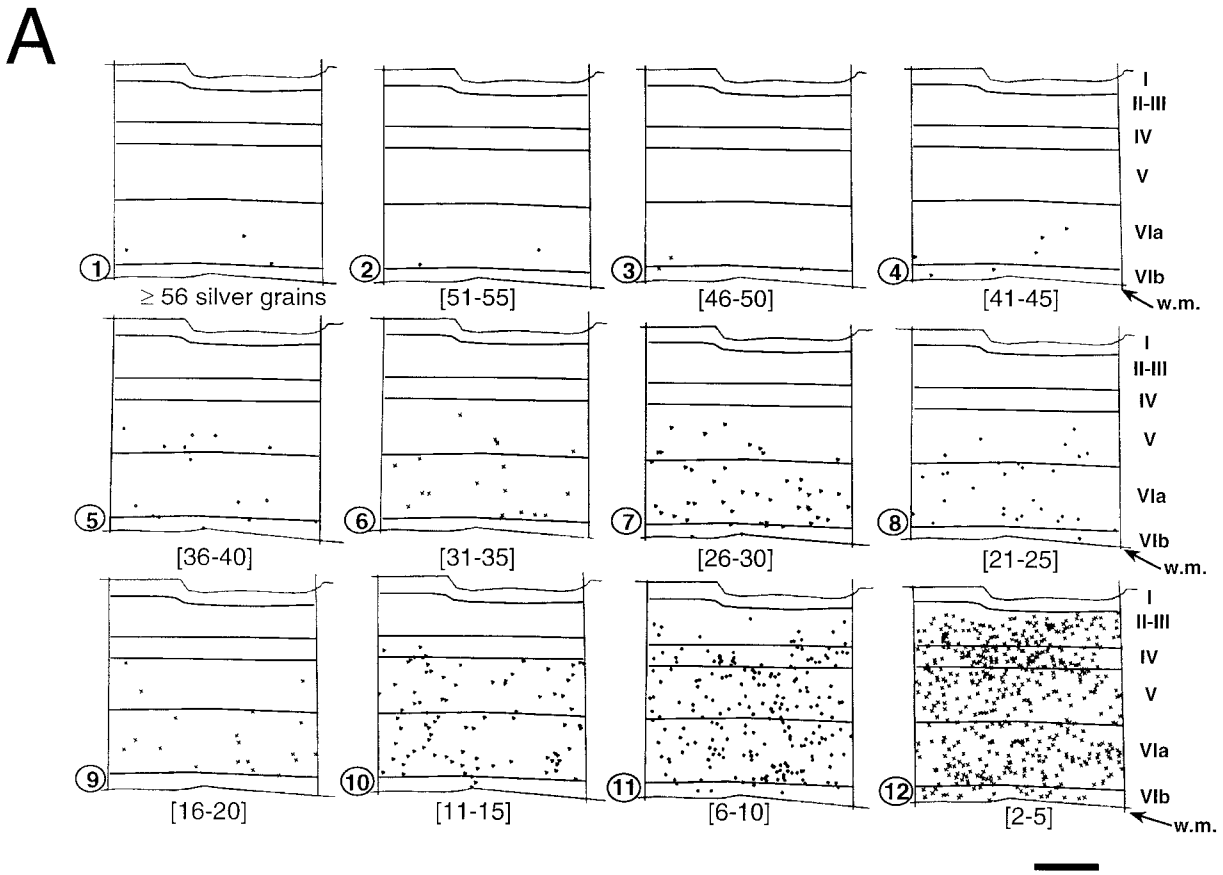

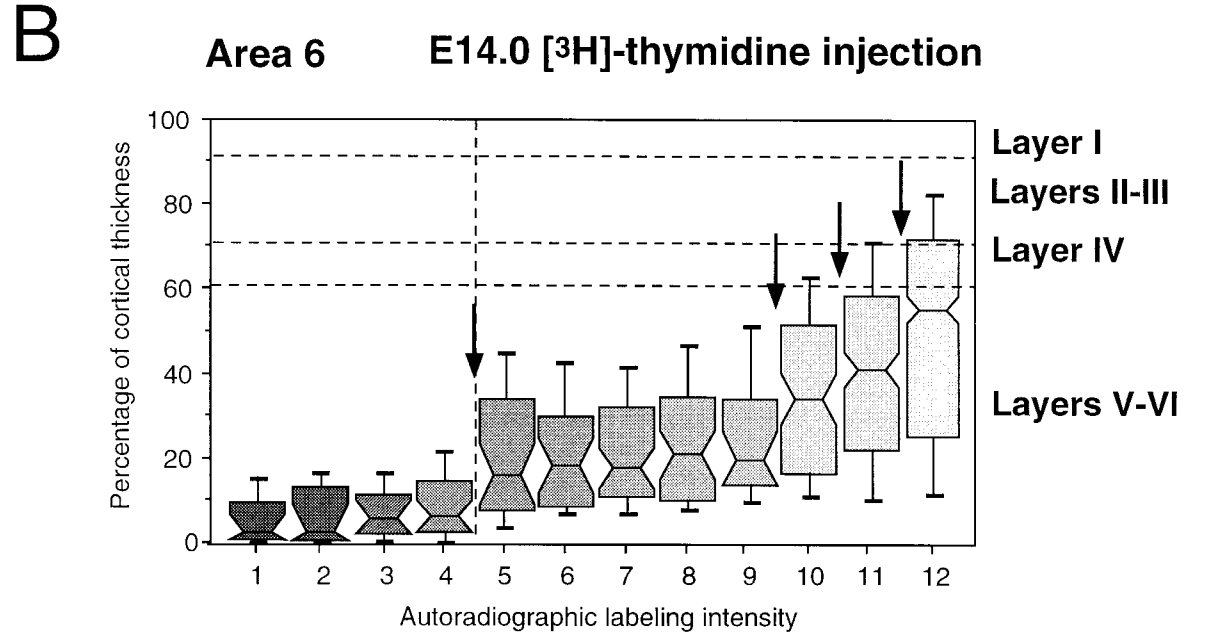

Fig. 3. Relationship between the intensity of autoradiographic labeling and radial location of area 6 neurons labeled by an E14 [^{3}H]thymidine pulse. **A:** Each panel shows the radial distribution of a category of labeled neurons defined by the numbers of silver grains per nucleus. **B:** Box plots of intracortical depth of different categories of labeled neurons. Each numbered box corresponds to a panel in A. This analysis has been performed on 993 labeled neurons in six nonadjacent sections taken from three different mice. For each box plot, the upper and lower thick lines indicate, respectively, the 90th and the 10th percentiles. Horizontal lines composing each box represent from top to bottom, respectively, the 75th, 50th (median), and the 25th percentiles. The choke indicates a 95% confidence interval around the median. The four inflections indicated by arrows have been detected by using a nonparametric Kolmogorov-Smirnov analysis (see Materials and Methods). Each arrow points to significant ($P < 0.05$) differences between the radial distributions observed for two adjacent categories of labeled neurons. This analysis shows that the first major cut-off corresponds to 50% maximal labeling between groups 4 and 5, which therefore identifies the first generation neurons. Abbreviations: w.m., white matter/grey matter boundary. Scale bar = 300 microns in A.

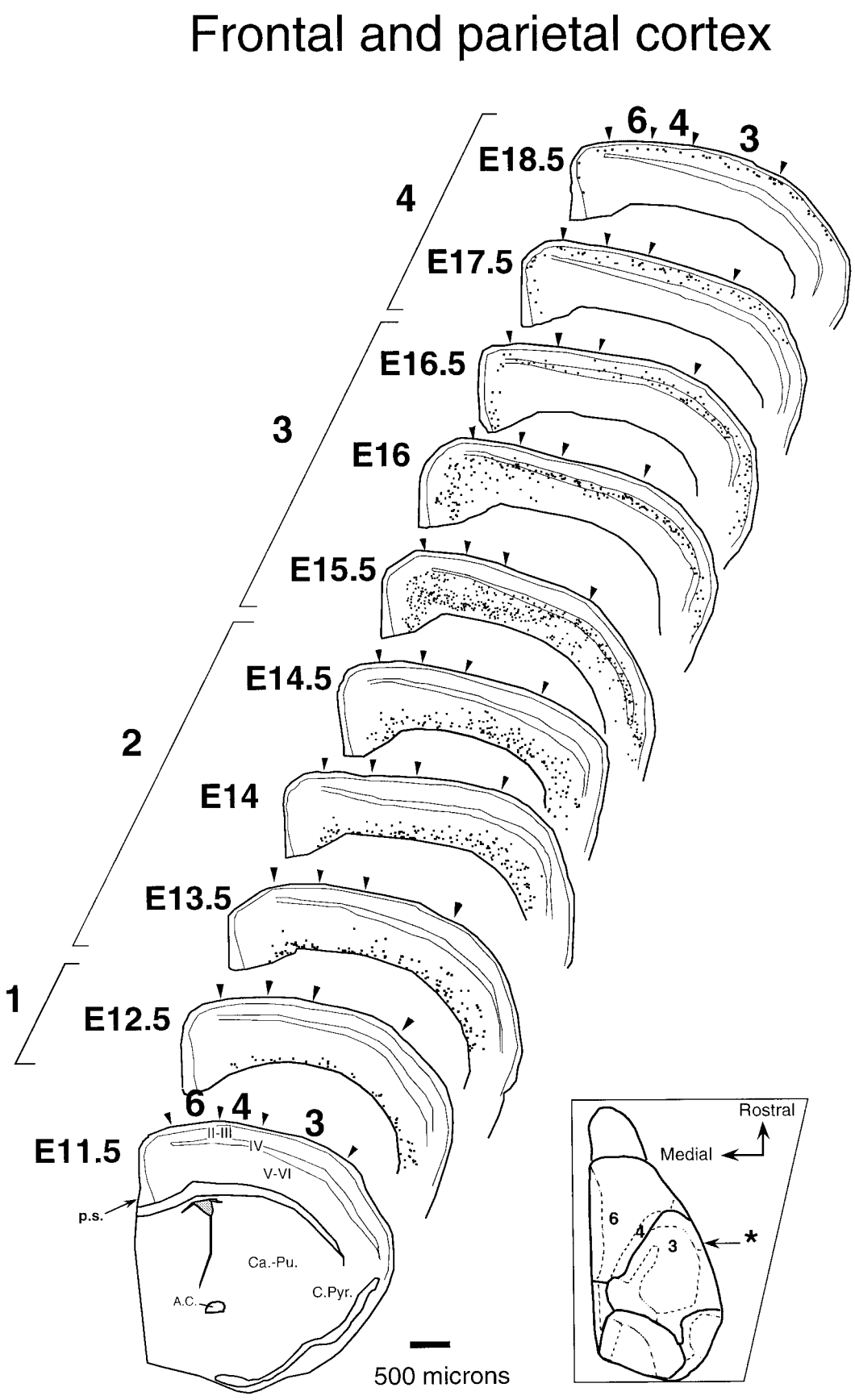

Fig. 4. Distribution of first generation (FG) neurons in frontoparietal cortex after injections on embryonic dates spanning the entire period of corticogenesis. On each plot, arrowheads indicate the positions of areas 6, 4, and 3. The **insert** indicates the approximate rostrocaudal level of sections examined. The star shows level of section. The shaded area represents the lateral ventricle. Abbreviations: Ca.-Pu., caudate putamen; A.C., anterior commissure; C.Pyr., pyriform cortex; p.s., pial surface.

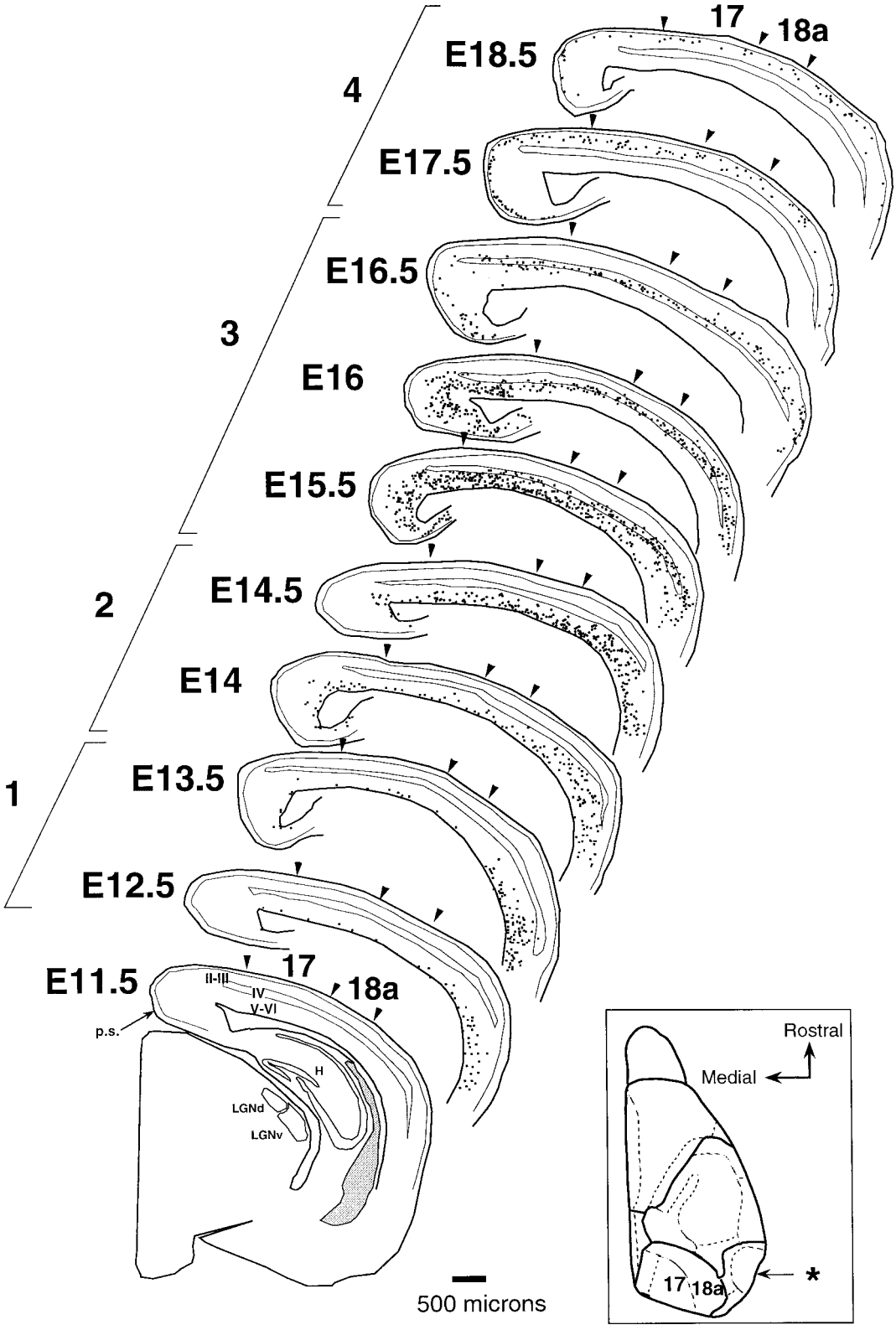

Fig. 5. Distribution of FG neurons in occipital cortex after injections on embryonic dates spanning the entire period of corticogenesis. On each plot, arrowheads indicate the relative position of areas 17 and 18a. Neurogenesis starts at the same time in areas 17 and 18a (E12.5) and also ends at the same time (E18.5) in these two areas. Despite obvious lateromedial and rostrocaudal neurogenic gradients, there is no clear difference of laminar distribution of FG neurons between areas 17 and 18a. Abbreviations and conventions as in Figure 4. LGNd and LGNv, dorsal and ventral part of the lateral geniculate nucleus, respectively; H, hippocampus.

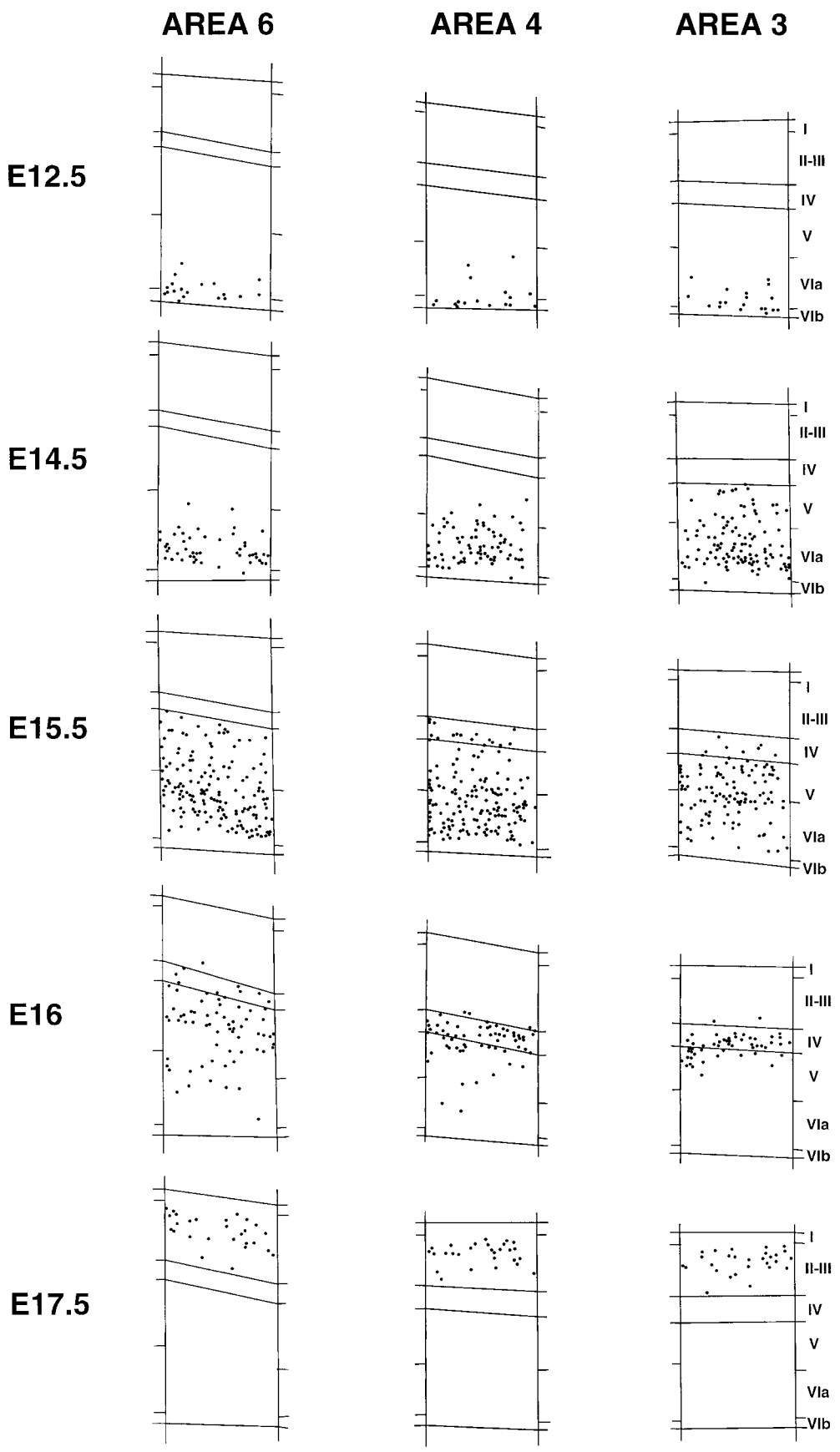

Fig. 6. Laminar distribution of first generation (FG) neurons in areas 3, 4, and 6. Each plot is prepared by cumulating the FG neurons on four 500-micron-wide strips on a total of four sections (two nonadjacent sections from two animals). These plots show that FG neurons are radially restricted and indicate areal differences.

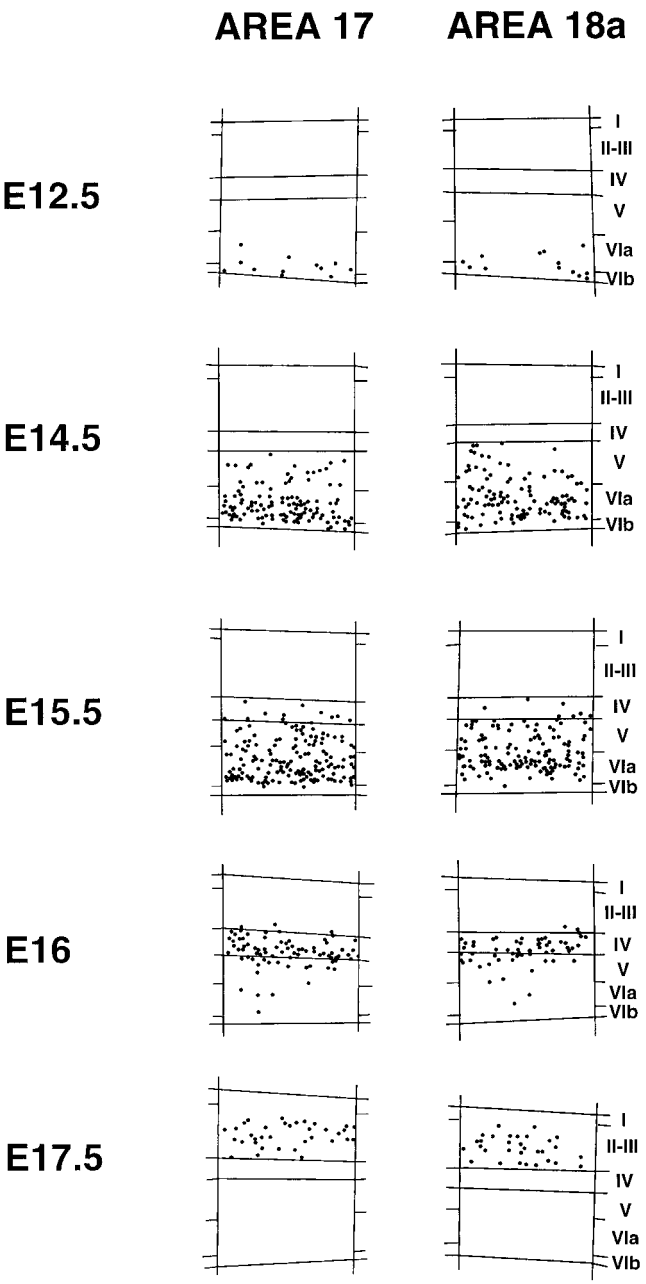

Fig. 7. Laminar distribution of first generation (FG) neurons in areas 17 and 18a. Each plot is prepared by cumulating the FG neurons on four 500-micron-wide strips on a total of four sections (two nonadjacent sections from two animals). This figure shows the similarity of the laminar distribution of FG neurons observed between areas 17 and 18a throughout cortical neurogenesis.

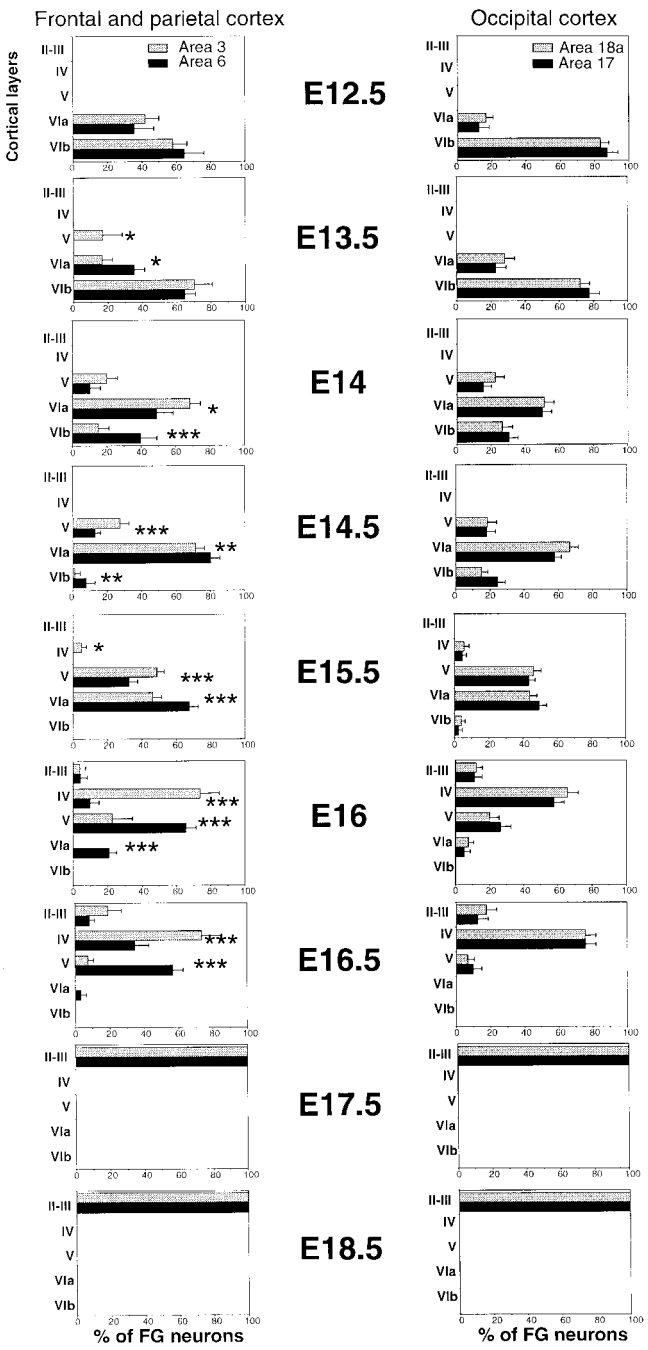

Fig. 8. Quantitative comparison of the laminar distribution of first generation (FG) neurons in separate cortical areas throughout cortical neurogenesis. Histograms show mean (±SEM) percentage of FG neurons per layer. Mean values have been calculated on the sections examined for the quantitative estimation of [FG/T] ratios (see Fig. 9). T, total number. Statistical analysis: single asterisk indicates $P < 0.05$, double asterisks indicate $P < 0.01$, and triple asterisks indicate $P < 0.001$, according to the χ^2 analysis (see Materials and Methods).

FG neurons in each layer of areas 3, 6, 17, and 18a for all 10 injections (area 4 has been left out so as to reduce the complexity of the figure) (Fig. 8).

In occipital cortex, the laminar distribution of neurons sharing a common birthdate was similar in areas 17 and 18a. The maximal percentage difference between these areas was generally less than 10% and there was no statistical difference in the proportions of FG neurons in each layer. This contrasted with the laminar distribution in frontoparietal cortex. For instance, whereas at E13.5 the entire neuron output in area 6 is devoted in the adult to layers VIa and VIb, nearly 20% of the neurons generated on this day in area 3 come to reside in layer V. Similarly on E16, neuron production in area 3 is almost entirely

devoted in the adult to layers V, IV, and to a small extent layers II-III, whereas a fifth of the output in area 6 is destined for layer VIa. At E16 nearly 80% of the output is destined in the adult for layer IV, whereas in area 6 less than 10% of neurons born on this day are destined for this layer. Likewise, generation of layer V (E14 and E14.5) is nearly twice as high in area 3 compared with area 6. The apparent heterogeneity of the laminar distribution of neurons sharing common birthdates in early stages of corticogenesis contrasts with the restricted deployment of neurons in the final stages of corticogenesis: all neurons produced in all five cortical areas from E17.5 to E18.5 are destined in the adult to reside in layers II-III and at no stage are there significant areal differences in the proportions of postmitotic neurons destined for these layers.

Laminar labeling index (FG/T)

Although cumulative plots of labeled neurons (Figs. 6 and 7) as well as the analysis shown in Figure 8 are suggestive of differences in onset of production of a particular layer, the areal difference in labeling could be the consequence of cell death, occurring either in the cortical plate or in the ventricular zone (see Discussion). Furthermore, areal differences of labeled cells in homologous layers could merely reflect differences in neuronal densities found in these layers in the adult. Hence, to be able to detect reliably differences in the laminar frequency of labeling in individual layers it is necessary to compute a relative measure of the number of FG neurons in each layer. To do this, we determined the FG/T ratio (where T equals the total number of labeled and unlabeled neurons in the layer).

FG/T has been used by several authors to measure rates of neurogenesis (Rakic, 1973; Mustari et al., 1979; Reznikov, 1990; Valverde et al., 1995). Use of this measure makes it possible to overcome any bias due to areal differences in cell density as well as differential cell death, because cell death will affect equally labeled and unlabeled neurons. Changes in FG/T are related to the rate of generation of a structure and Rakic (1973) referred to this as a generation rate. When applied to layer formation FG/T provides a relative measure of the rate of production of the layer at the moment of injection (see discussion).

The present study aims to assess interareal differences. We have made these comparisons between areas on the same rostrocaudal level, so that the areas being compared were separated uniquely by a lateromedial distance. We have ensured that the distance separating radial strips in areas 3 and 6 was exactly equivalent to that separating radial strips in areas 17 and 18a.

FG/T values returned by pulse injections throughout the period of formation of a cortical layer enable us to evaluate accurately changes of laminar generation rate during development (Fig. 9). The laminar generation curves in Figure 9 provide a quantitative comparison of the production of the individual cortical layers in areas 3, 4, 6 (left-hand side) and in areas 17 and 18a (right-hand side). This analysis reveals important differences in FG/T values between areas 3, 4, and 6 before the arrival of thalamic afferents in the vicinity of the cortex at E15.5 (indicated by vertical grey bar) (Bicknese et al., 1994; Cohen-Tannoudji et al., 1994; Molnar and Blakemore, 1995; Polleux et al., 1996). This finding contrasts with findings in the occipital cortex in which FG/T values at all stages were very similar.

Cortical neurogenesis starts synchronously in all three frontoparietal areas by layer VIb production, which begins shortly after E11.5, peaks at E13.5, and is terminated by E15.5. FG/T values of layer VIb for all three parietal areas overlap at all ages.

The synchronous onset of layer VIa production in all three frontoparietal areas occurs at E12.5 and FG/T values for this layer remain identical in all areas up to E13.5. The major phase of neuron production of layer VIa occurs earlier in areas 3 and 4 than in area 6 so that from E14 to E14.5 FG/T values are nearly twice as high in layers VIa of areas 3 and 4 compared with area 6. There is a simultaneous rapid decline in FG/T values in layer VIa in all three areas and production of this layer is complete by E16.5.

In frontoparietal areas, the onset of neuron production of layer V occurs simultaneously in areas 3 and 4 at E13.5 and 12 hours later in area 6. From E14–E15.5, FG/T values of layer V are considerably higher in area 3 than they are in areas 4 and 6. At E16, values for layer V drop in area 3, and production is terminated by E17.5. FG/T values for layer V in areas 4 and 6 peak at E15.5 and are maintained at E16. Production of layer V in all three areas terminates at E17.5.

The onset of layer IV production at E15.5 and E16 is significantly higher in areas 3 and 4 compared with area 6. There is a rapid decrease in layer IV production in all three areas after E16.5, and production of this layer, like that of the infragranular layers, is terminated by E17.5. Finally, the onset, duration, and relative rate of neuron production of layers II-III in frontoparietal areas are identical so that their laminar generation curves overlap.

In contrast to frontoparietal areas, the laminar generation curves for all layers in areas 17 and 18a overlap, indicating a high synchrony in the onset, duration, and relative rate of laminar generation of these two occipital areas.

These results reveal significant differences between all three frontoparietal areas, particularly between areas 3 and 6. These important differences are unlikely to merely reflect known lateromedial gradients given that the same separation was set between areas 17 and 18a and between areas 3 and 6 and given that FG/T values in areas 17 and 18a did not differ (Fig. 9).

So as to be able to compare better the timetable of laminar production in each area, best fit curves were calculated for the laminar generation curves. Cut-off points at 10% of peak value gave estimations of onset and termination of layer production (Fig. 10). Onset of cortical neuron production occurs in all five areas within a 4-hour window around E11.5. Onset of homologous cortical layers in different areas was on average within a 8-hour period (range, 4–13 hours). Interestingly, the maximum delay in layer production in neighbouring frontoparietal areas was larger than that between distant areas situated in occipital and frontoparietal cortices. The maximum delay within frontoparietal areas was in the onset of generation of layers V (10 hours) and IV (12 hours). The maximum delay between occipital and frontoparietal areas was 8 hours in the onset of layer V. There was a tendency for the onset of production of a particular layer in occipital cortex to be closer to the onset of that layer in area 3 than the same layer in area 6. The termination of layer production was rather synchronous between the different areas except for VIb, which lasted nearly 30 hours longer in occipital cortex compared with frontoparietal areas.

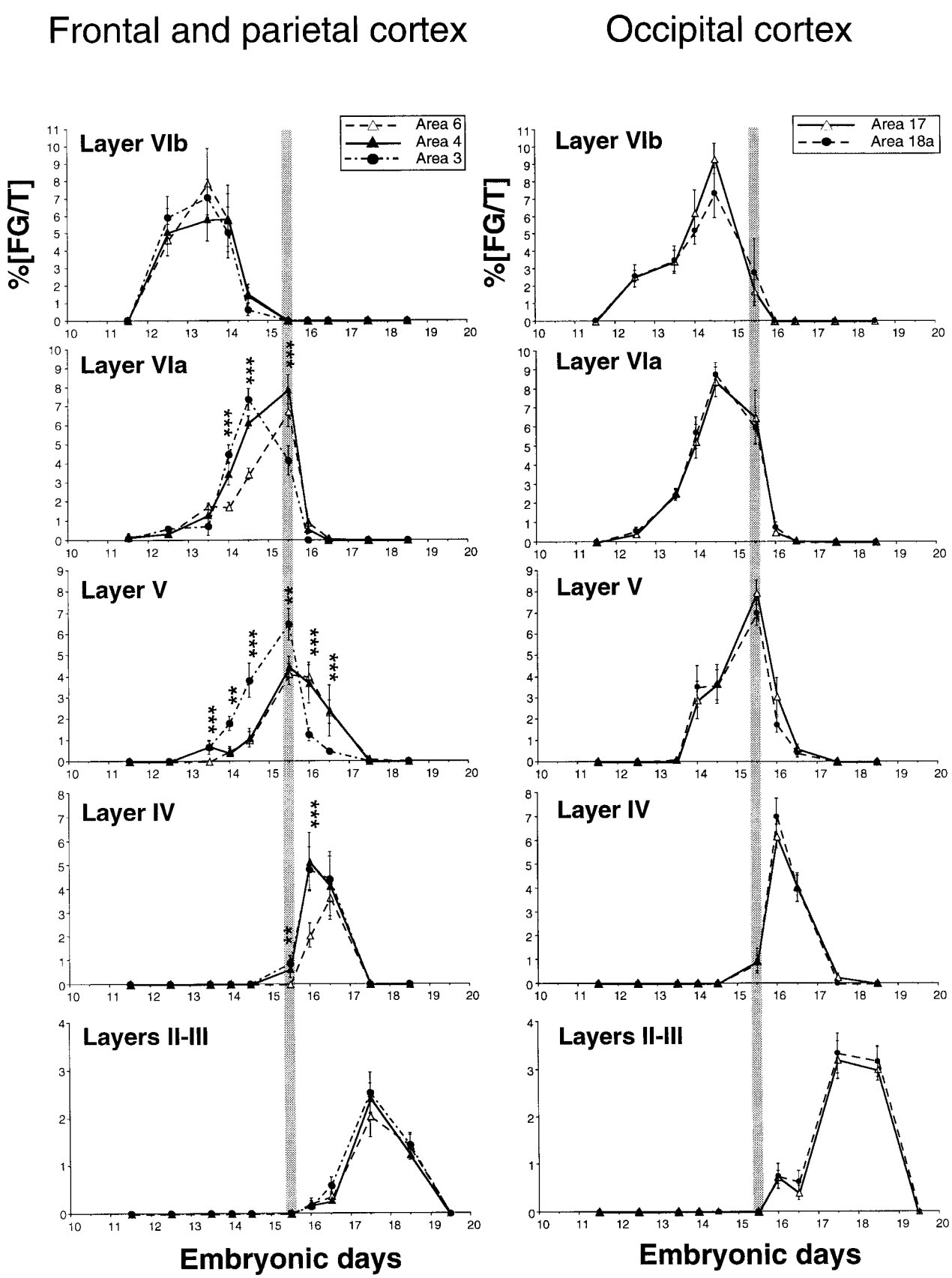

Fig. 9. Laminar labeling index [FG/T].This analysis demonstrates that frontoparietal areas are characterised by significant differences in the timetable of infragranular and granular layers production. Despite being separated by the same lateromedial distance as areas 6 and 3, areas 17 and 18a are characterised by identical FG/T curves. Error bars represent one standard error of the mean. Statistical analysis: single asterisk indicates $P < 0.05$, double asterisks indicate $P < 0.01$, and triple asterisks indicate $P < 0.001$, according to the χ^2 analysis (see Materials and Methods). Vertical grey line: arrival of thalamic afferents (see text).

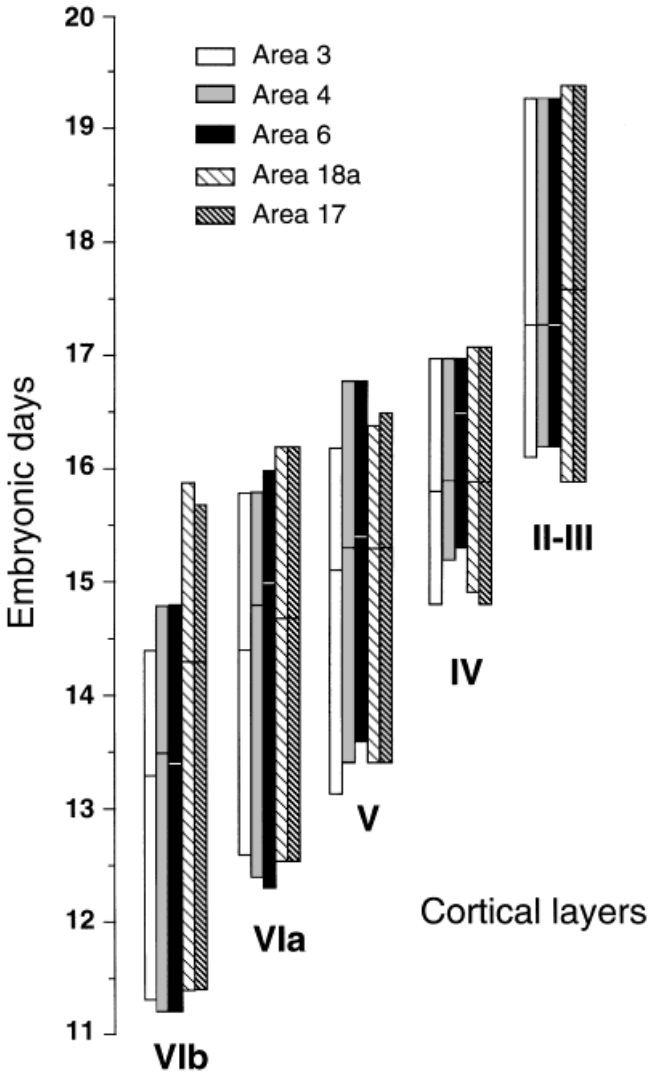

Fig. 10. Timing of laminar generation of areas 3, 4, 6, 17, and 18a. Each vertical bar is proportional to the duration of production of the cortical layer indicated. The estimated peak of neurogenesis is indicated by a small horizontal bar. The onset, peak, and offset of production have been estimated from the experimental mean values of [FG/T] percentages in Figure 9 by means of a best fit curve analysis (performed by using KaleidaGraph™ v. 2.1.4 software [Deltasoft]). The onset and end of production correspond to 10% of peak values.

Peak values of the laminar generation curves showed significant differences in timing in homologous layers of different areas. The timing of peak production showed maximal differences within frontoparietal areas. Peak FG/T values in layers VIa and IV of area 6 lagged 15 and 18 hours behind the homologous layers of area 3. The maximum difference between occipital and frontoparietal areas was of the order of 24 hours in peak rates of layer VIb production. Elsewhere peak production in occipital cortex was within a maximum of 7 hours after peak production of the homologous layer in area 3.

Are interareal differences larger than intra-areal differences?

This question is a crucial issue because we need to distinguish abrupt differences at areal limits from smooth, progressive differences within areas that are expected to result from known lateromedial and rostrocaudal neurogenic gradients. To address this issue we have (i) verified that there is a simultaneity both in the onset and offset of neuron production throughout isocortex (Fig. 11) and (ii), we have compared laminar histogenesis of layer IV at three distant loci within each area (Figs. 12 and 13).

At E12.5 the first generated neurons appear simultaneously in layer VIb across all five areas, and no differences in the density or radial location of FG neurons can be detected at any rostrocaudal position (Fig. 11). Note that at this and at subsequent ages, labeled neurons are more numerous and higher in the cortex regions lateral to area 3, confirming a lateromedial gradient of neurogenesis. However, this lateral region is clearly outside of the dorsofrontal and occipital regions where we have carried out interareal comparisons and corresponds mainly to limbic cortex (Caviness, 1975).

The last neurons to be generated are on E18.5, where once again there is no difference in the density or radial location of labeled neurons at different lateromedial and rostrocaudal positions (Fig. 11).

Areal differences in the radial location of [^{3}H]thymidine labeled neurons in and around layer IV after injections on E15.5 and E16 are illustrated in Figure 12. At E15.5 labeled neurons are present in layer IV in area 3 (level B and C) but are absent in layer IV in area 6 (level A and B). Labeled neurons are present in layer IV at all levels in areas 17 as well as in area 18a (levels D and E). This result shows that the clear and characteristic delay in the generation of layer IV in area 6 is found at all lateromedial and rostrocaudal positions.

At E16 a few labeled neurons begin to appear in layer IV in area 6, whereas in areas 3, 4, 17, and 18a nearly all neurons born on this day are destined for layer IV. Hence, infragranular layer production is largely terminated in areas 3, 4, 17, and 18a, whereas the production of these layers persists in area 6 (Fig. 12, see also Fig. 9).

By calculating the value of FG/T for layer IV we can compare quantitatively the rate of production of this layer between areas and different positions within areas (Fig. 13A). In this figure the levels A to E are the same as in Figures 11 and 12. At level A, medial and lateral levels of area 6 are found to have identical rates of layer IV production from E15.5 to E17.5. Similarly, identical rates of layer IV production were found in lateromedial separations in area 3 from E14.5 to E17.5 (level C) and in area 17 from E14.5 to E17.5 (level E). This analysis confirms that generation of layer IV starts approximately 12 hours later in area 6 than in areas 3, 17, and 18a. Note that layer IV follows a similar timetable in areas 4 and 3 (Fig. 9). Also note that the peaks in FG/T values do show a transition from E16 at rostral levels of area 6 (level A) to E16.5 at caudal levels of area 17 (level E) reflecting a weak rostrocaudal gradient.

The similarity of FG/T values at different loci within areas justifies pooling lateromedial and rostrocaudal values for areas 3 and 6 (Fig. 13B). This confirms that there is a significant delay in the onset of layer IV production in area 6 compared with area 3.

DISCUSSION

The present results provide an areal comparison of the chronoarchitecture of the mouse isocortex. By distinguishing different categories of [^{3}H]thymidine labeled neurons

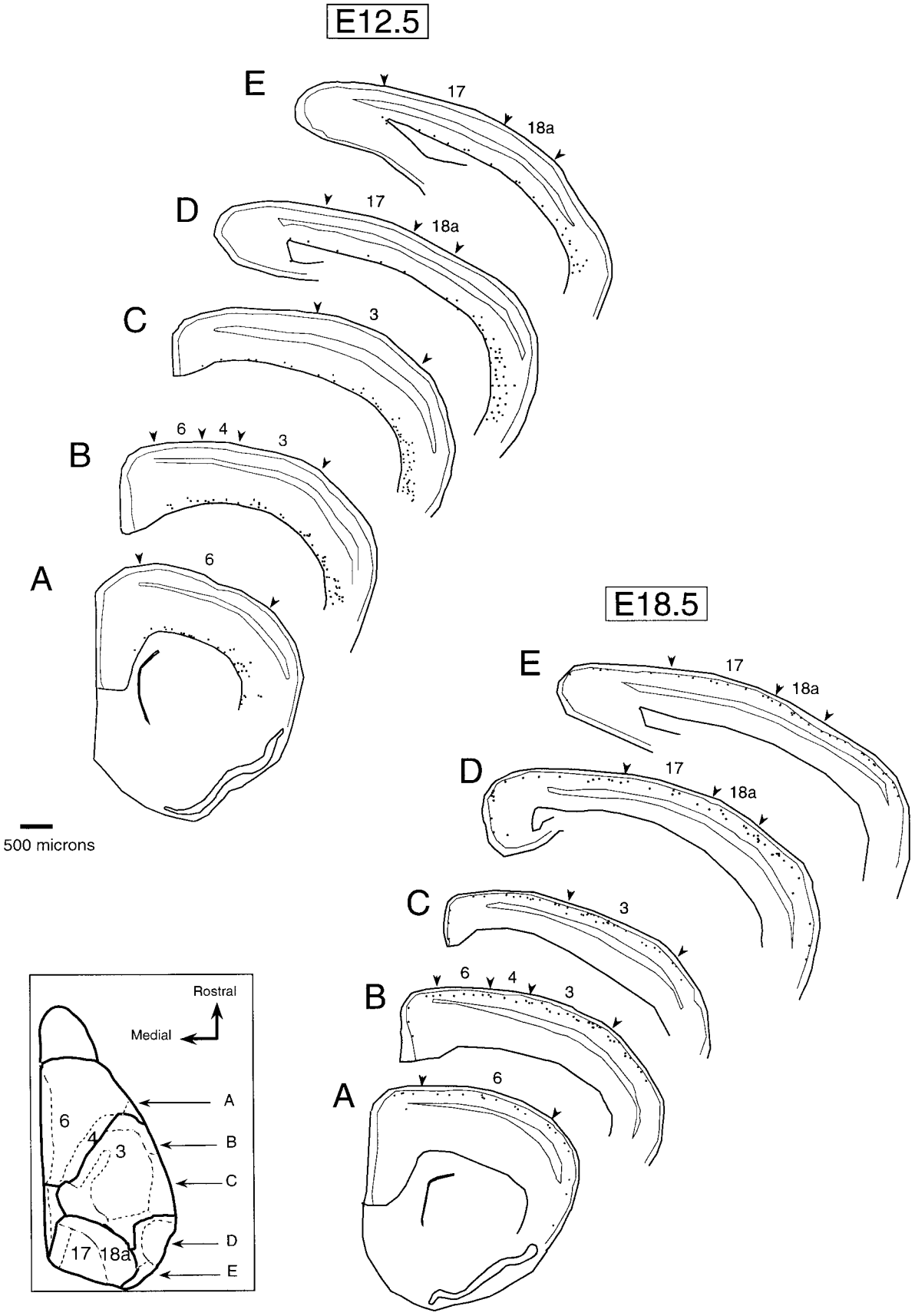

Fig. 11. Comparison of laminar distribution of first generation (FG) neurons during the onset (E12.5) and the offset (E18.5) of cortical neurogenesis on coronal sections spanning the entire rostrocaudal extent of mouse isocortex. The rostrocaudal level of the coronal sections (**A–E**) is indicated in an **insert** on a dorsal view of mouse isocortex modified from Caviness (1975). These plots of FG neurons show that neurogenesis starts and terminates synchronously throughout the entire isocortex. Same conventions as in Figures 4 and 5.

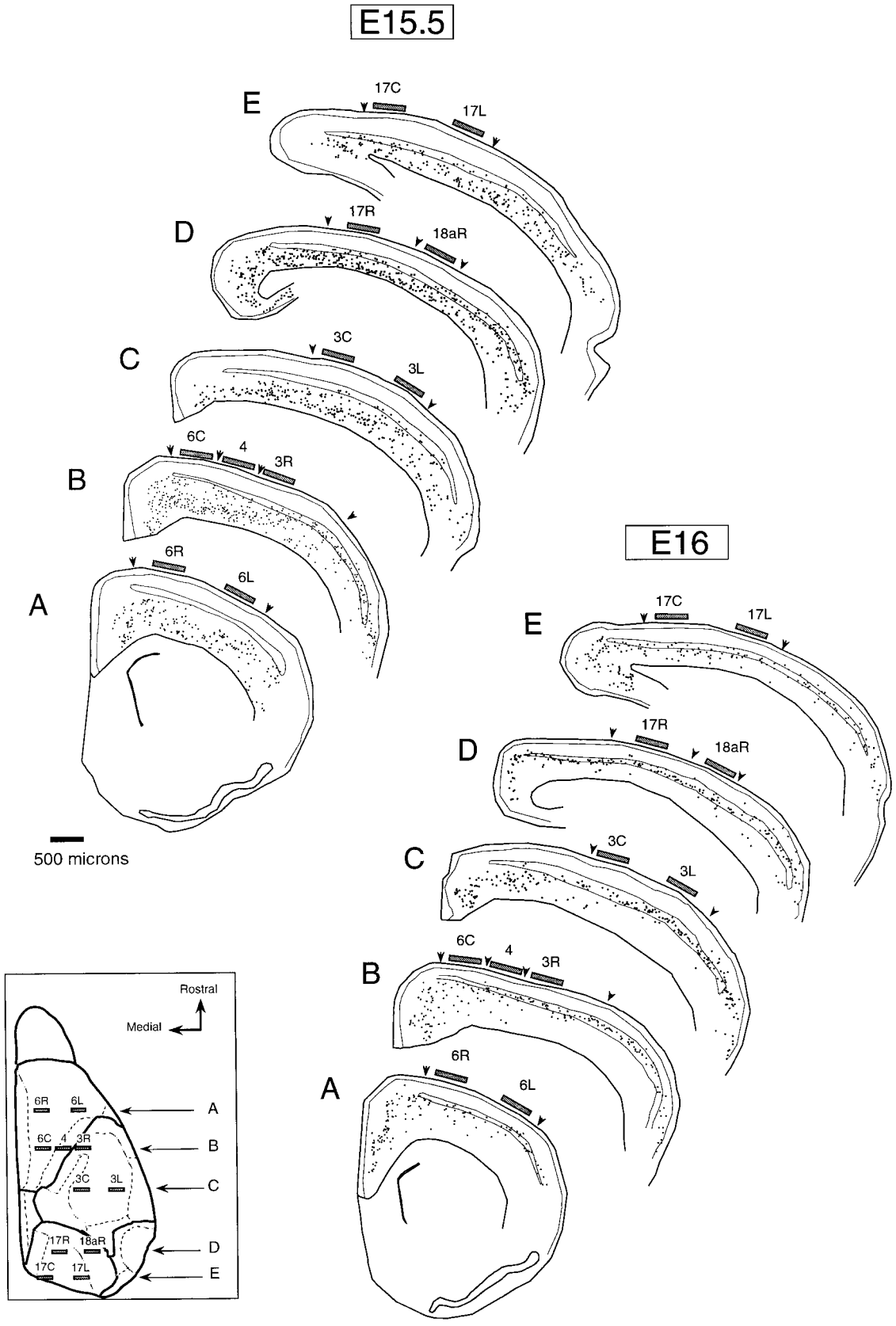

Fig. 12. Comparison of laminar distribution of first generation (FG) neurons within and between cortical areas. The rostrocaudal level of the coronal sections (**A-E**) is indicated in an **insert** (same conventions as in Fig. 2). On each plot and on the insert, the shaded bars indicate the location of the cortical regions analysed quantitatively in Figure 13. This comparison shows that despite known neurogenic lateromedial and rostrocaudal gradients, the laminar distribution within areas is fairly constant and that the major differences in the laminar location of FG neurons occurs between areas. Abbreviations: 17C: caudal part of area 17; 17R: rostral area 17; 17L: lateral area 17; 18aR: rostral area 18a; 3C: caudal area 3; 3R: rostral area 3; 3L: lateral area 3; 4: area 4; 6C: caudal area 6; 6R: rostral area 6; 6L: lateral area 6.

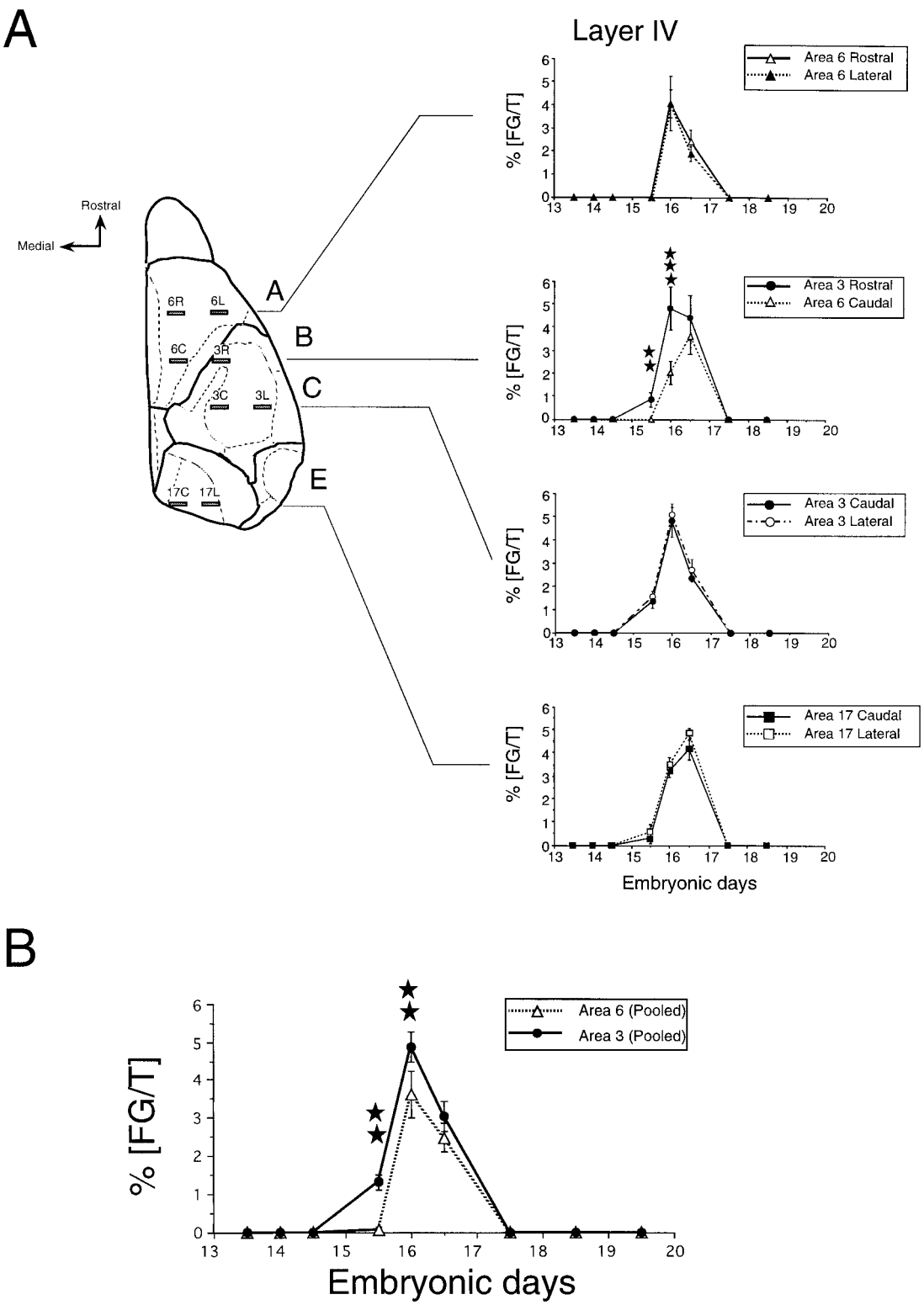

Fig. 13. Quantitative analysis of layer IV production within and between areas 6, 3, and 17 by using the laminar labeling index FG/T. **A:** The left-hand part of the figure indicates the position of the cortical regions analysed in this figure on a dorsal view of mouse isocortex (same conventions as in Fig. 2). Note that each pair of lateromedially separated cortical regions (respectively, from rostral to caudal: 6R-6L, 6C-3R, 3C-3L, 17C-17L) are separated by the same lateromedial distance so as to be able to compare the effect of lateromedial neurogenic gradient on layer IV production between and within these cortical areas. The right-hand part of the figure shows FG/T curves calculated in layer IV at the four rostrocaudal levels indicated in the inset. This analysis shows that there is no apparent effect of the lateromedial neurogenic gradient on the timetable of layer IV production within area 6, 3, or 17 at the distance used in the present study (600–700 microns). This finding contrasts with the highly significant differences observed between areas 6 and 3 (level B). **B:** Global values of FG/T have been calculated by pooling values obtained from each of the three levels (A, B, and C, shown in A) analysed in areas 6 and 3. This finding confirms that production of layer IV in area 6 is delayed with respect to area 3. Error bars represent one standard error of the mean. Statistical analysis: double asterisks indicate $P < 0.01$, triple asterisks indicate $P < 0.001$, according to the χ^2 analysis (see Materials and Methods).

we have been able to quantitatively correlate the radial location of labeled neurons and labeling intensity. This approach has enabled us to define labeling criteria that identify the cohort of neurons which quit the cell-cycle during a narrow window of time after the first mitosis following the [^{3}H]thymidine pulse. Cumulative plots of labeled neurons suggest differences in the timetable of layer production in adjacent areas of the frontoparietal cortex. Changes in FG/T provide a detailed description of the onset, duration, and relative rate of layer production and confirm that there are indeed important differences between homologous layers in the different frontoparietal areas examined. A quantitative areal comparison of laminar production shows that between E14 and E16, neighbouring frontoparietal areas generate different proportions of infragranular and granular layers. These areal differences are superimposed on known neurogenic gradients. However, comparisons of timetable differences at different loci within areas reveal only very minor differences compared with the large and abrupt changes between areas.

Can temporal and spatial patterns of histogenesis be inferred from cortical labeling in the adult?

Detection of autoradiographic signal. Although the number of silver grains overlying the nucleus is related to the amount of [^{3}H]thymidine, in a number of instances it is an underestimation (Rogers, 1967; Sidman, 1970). There are two categories of errors. (i) Physical constraints of the autoradiographic technique: these errors are mainly due to the fact that β particles have a limited penetration so that nuclei that are deep in the section will show artifactually lowered numbers of silver grains (Sidman, 1970). (ii) Biological limitations: a number of FG neurons will show artifactually weak [^{3}H]thymidine labeling because their progenitors were at the end or beginning of S-phase at the moment of the pulse (Bisconte and Marty, 1975). Both categories of errors will lead to an underestimation of the laminar generation rates and the duration of layer formation. However, neither category can induce significant interlaminar variations, which would be needed to alter the main conclusions of the present study. Physical constraints could only lead to a laminar variation if there were significant differences in the nuclei size in the layers compared. This problem can be discarded in the present study because the important comparisons in generation rates are made for homologous layers and therefore between classes of cortical neurons that have a similar range in sizes (Beaulieu, 1993). The biological limitations could lead to an artifactual laminar variation of FG values if there were large variations in S-phase between layers. However, this is unlikely to be the case because S-phase duration shows little change during corticogenesis (Schmahl, 1983; Takahashi et al., 1995).

Differential cell death. Naturally occurring cell death is known to occur both prenatally and postnatally in the developing rodent cortex as well as amongst the neuronal precursors in the germinal zones (Finlay and Slattery, 1983; Heumann and Leuba, 1983; Ferrer et al., 1990; Soriano et al., 1993; Ferrer et al., 1994; Reznikov and van der Kooy, 1995; Spreafico et al., 1995; Blaschke et al., 1996). If such levels of cell death were to specifically affect particular layers in individual areas they could generate areal differences in the numbers of labeled neurons. For instance, if a radially restricted category of neurons were to die in the cortex or a temporally restricted wave of precursors were to die in the germinal zones then this could lead to areal differences in the numbers of labeled neurons in homologous layers. For this reason, cell death could be responsible for the differences in the cumulative labeling of homologous layers shown in Figure 6. It is therefore necessary to use the laminar FG/T value to determine areal differences in the timetable of layer formation. It needs to be emphasised that laminar FG/T values cannot be artifactually affected by cell death. This is because, in the event of a temporally restricted wave of cell death in the ventricular zone, this phenomenon will concern equally labeled and unlabeled precursors. Likewise in the event of a spatially restricted wave of cell death in the cortical plate or immature cortex labeled and unlabeled neurons within a given cortical layer will be equally affected.

Radial versus tangential migration. According to the radial unit hypothesis, the areal location of neurons in the cortex is determined by their point of origin in the ventricular zone and therefore requires that migration from the ventricular zone to the cortical plate be predominantly radial (Rakic, 1988). A number of recent cell lineage studies using retroviral-mediated labeling or transgene expression by precursors in the ventricular zone have detected variable amounts of tangential dispersion of clonally related neurons going from a few hundred microns (Luskin et al., 1988; Price and Thurlow, 1988; Moore and Price, 1992; Luskin et al., 1993; Soriano et al., 1995) to several millimeters (Austin and Cepko, 1990; Walsh and Cepko, 1992; Reid et al., 1995). However, some of the tangential dispersion demonstrated by these lineage studies concerns migration of precursors and therefore is not at odds with a predominantly radial migration (Reid et al., 1995). Some tangential dispersion has been reported in mice where cellular mosaicism can be visualised in cortex after random inactivation of an X chromosome-linked *lacZ* transgene (Tan and Breen, 1993; Tan et al., 1995). Lastly, a number of studies have observed tangential migration either dynamically using time-lapsed confocal microscopy (O'Rourke et al., 1992) or indirectly using more conventional histological techniques (O'Rourke et al., 1995).

Clearly, if tangential displacement were to contribute to a large extent to the translocation of postmitotic neurons, this will invalidate the use of [^{3}H]thymidine labeling in the cortex as a means of inferring developmental events in the underlying ventricular zones. Rakic (1995)has attempted to estimate the overall extent of tangential migration using the data generated by Tan et al. (1995). These authors showed that there is a mosaic expression of a reporter gene leading to radial columns of β-galactosidase positive (β-gal(+)) cells in the cortex. That there is a mixing of β-gal positive and negative cells implies a fair degree of tangential movement of migrating postmitotic neurons. However, the degree of mixing can also be used to estimate the extent to which tangential migration contributes to the overall displacement of immature neurons. It can be argued that, if tangential migration occurred massively, then there would be a randomisation of β-gal(+) cells in the cortex and there would be no radial patterns of labeling. In this way it can be calculated that less than 10% of immature cortical neurons undergo tangential migration (Rakic, 1995).

Possible mechanisms generating areal differences in the timetable of laminar genesis. The principal aim of the FG/T calculation in the present study is to obtain a reliable indication of the onset and termination of layer production in five different cortical areas. These differences in the timetable of layer production could be the consequence of an areal difference in recruitment and/or in proliferative mechanisms.

Recruitment. The most important control of the timing of layer production is likely to be the environmental signalling in the ventricular zone (McConnell, 1988; McConnell and Kaznowski, 1991). Pulse injections of [^{3}H]thymidine at the very onset of layer formation return low FG/T values. As time progresses the FG/T values steadily increase, reach a peak value, and then decrease. This generation curve largely reflects the fact that cells undergoing their final mitosis at a given moment are not destined for a single, restricted strata of the cortex nor even a single cortical layer (Angevine and Sidman, 1961; Berry and Rogers, 1965; Hicks and D'Amato, 1968; Fernandez and Bravo, 1974; Rakic, 1974; Smart and Smart, 1977; Caviness, 1982; Smart and Smart, 1982; Luskin and Shatz, 1985; Jackson et al., 1989; Sanderson and Weller, 1990; Bayer and Altman, 1991; Dehay et al., 1993). Instead, the population of labeled neurons peaks at a given radial height in the cortex (determined by the embryonic age at injection) and tails off smoothly above and below this peak into adjacent layers. Hence, areal differences in laminar FG/T values will be largely determined by differences in the recruitment of precursors to the production of the layer in question. According to current theories, these areal differences in recruitment would be in response to differences in environmental signalling (McConnell, 1988; McConnell and Kaznowski, 1991; Frantz and McConnell, 1996).

Proliferation. Amongst a population of precursors recruited to the formation of a layer, changes in rates of proliferation can directly contribute to the rate of layer formation. Areal differences in the peak values of generation curves could theoretically reflect areal differences in proliferation kinetics. This raises the complex issue of the theoretical significance of labeling indices in general and FG/T in particular. In the present study we have examined the labeling indices (FG/T) in the adult cortex, and we need to address the relevance of this adult measure to understanding developmental events.

In the ventricular zone, the proportion of precursors labeled by a [^{3}H]thymidine pulse is directly related to the relative duration of S-phase with respect to the overall duration of the cell-cycle (Fujita, 1963; Waechter and Jaensch, 1972; Schultze et al., 1974; Nowakowski et al., 1989). Because S-phase remains fairly constant during corticogenesis (Waechter and Jaensch, 1972; Schmahl, 1983; Takahashi et al., 1995), changes in the labeling index of a pool of precursors reflect predominantly changes in the duration of the cell-cycle. In this way, high labeling indices indicate fast cycle times and low indices long cycle times. After migration of the labeled and unlabeled postmitotic neurons, variation in FG of cortical neurons can reflect under certain conditions either a variation in the proportions of labeled precursors and/or the leaving fraction (Schultze et al., 1974; Bisconte and Marty, 1975; Brückner et al., 1976). We refer to changes in both of these parameters as changes in the kinetics of the cell cycle.

Although the present results do not allow us to directly address whether or not regional differences in cell-cycle kinetics contribute to the regionalisation of layer formation, the differences in the generation curves shown in Figure 9 give an indication that this may be the case. Differences of FG/T between two homologous layers in two areas have particular significance with regard to the possibility of differential proliferation mechanisms when two conditions are met: (i) when the majority of FG neurons labeled by the pulse are contained within the homologous layers; (ii) when the two layers have similar T values. Under these conditions, differences in FG/T come down to differences in the numbers of FG neurons in the two layers. This difference however cannot be generated by cell death (because the difference is maintained when FG is compared as a ratio of T). Under these conditions, differences in the numbers of FG neurons are either generated by differences in the cell-cycle kinetics or in the numbers of precursors. It should be kept in mind that differences in the numbers of precursors ultimately are derived from an earlier difference in cell-cycle kinetics during the establishment of the pool of precursors present at the moment of the [^{3}H]thymidine pulse.

The above criteria are met in the frontoparietal areas. T values are equivalent in layers VIa of areas 4 and 6 (Beaulieu, 1993; Skoglund et al., 1996). The peak FG/T value is to be expected when the [^{3}H]thymidine pulse is delivered midway in the formation of a layer. At E14.5, FG neurons in areas 4 and 6 are almost entirely restricted to layer VIa (Fig. 6) and the FG/T ratios at this age and for these layers are significantly different (Fig. 8). These findings in frontoparietal areas are compatible with but do not constitute first-hand proof of a proliferative mechanism contributing to differences in the rates of layer formation in different areas.

How do the present findings relate to known neurogenic gradients?

A number of studies have reported that lateral and frontal cortical regions are generated before medial and posterior regions (Shimada and Langman, 1970; Fernandez and Bravo, 1974; Raedler and Raedler, 1978; Raedler et al., 1980; Gardette et al., 1982; Smart and Smart, 1982; Schmahl, 1983; Miller, 1988; Sanderson and Weller, 1990; Bayer and Altman, 1991; Ignacio et al., 1995; Reznikov and van der Kooy, 1995). Although the present results showing areal differences in laminar generation rates are in agreement with previous claims of tangential neurogenic gradients, they also reveal a simultaneity in the onset of neurogenesis of distant areas across the rodent cortex (Bayer and Altman, 1991; Ignacio et al., 1995).

The present results allow an improved understanding of neurogenic gradients in the cortex. These results show that the generation of the cortex is characterised by a simultaneous onset of neuron release across the cortex. This onset is followed by a phase of sustained production and terminates by a relatively simultaneous cessation of neuron production in all areas. The sustained period of neuron production that takes place during midcorticogenesis is characterised by regional differences in the relative rate of laminar generation (FG/T). The differences in the relative laminar rates of neuron production revealed in the present study are largely compatible with neurogenic gradients described across cortical regions by other authors (Shimada and Langman, 1970; Fernandez and Bravo,

1974; Gardette et al., 1982; Smart and Smart, 1982; Sanderson and Weller, 1990; Bayer and Altman, 1991). The regional differences in histogenesis do not correspond to a moving wave, because this would generate similarly shaped laminar generation curves with a constant offset in each area. Rather, after the synchronous onset of corticogenesis of the first cortical layer (layer VIb), there are local variations in the relative rates of layer production. This leads to significant differences in the laminar FG/T values of homologous layers in the frontoparietal region (Fig. 9), which constitute differences in the onset, duration, and relative rate of individual layer formation (Fig. 10).

The present study shows that the infragranular and granular layers in area 6 are generated later than the homologous layers in area 3. Because area 6 lies medial to area 3, it could be argued that this simply reflects the known neurogenic gradients. However, the present findings show (1) that the differences between areas 3, 4, and 6 are abrupt changes, which occur at the areal borders, and (2) that these changes constitute a much more rapid change than that generated within any single cortical area or even across large stretches of cortex including several areas. These findings are illustrated in Figures 9 and 13, which show that two loci on either side of the area 3-4 border show approximately a 12 hours difference in the onset of layer IV production. This contrasts with the rostrocaudal gradient, which leads to a maximum of 12 hours difference in the location of the peak of layer IV production between the most rostral and the most caudal regions of the cortex (compare rostral area 6 with caudal area 17 in Fig. 13).

This result suggests that abrupt increases in neurogenic gradients can generate important interareal differences in the timetable of laminar histogenesis. This finding in the frontoparietal cortex of the mouse is comparable with the apparent differences in laminar histogenesis across the 17-18 border in the monkey (Dehay et al., 1993). Given the marked differences in the laminar distributions of [^{3}H]thymidine labeled neurons in areas 17 and 18 in the primate (Rakic, 1976; Dehay et al., 1993) and in the hippocampus of mouse (Angevine, 1965) and monkey (Rakic and Nowakowski, 1981), it could be hypothesised that areal differences in timetable of layer production is a common feature of the cerebral cortex.

In the primate neocortex, laminar histogenesis in the more caudal area, area 17, would seem to lag behind that of the more rostral area, area 18, and therefore is consistent with a rostrocaudal gradient. Like in the mouse frontoparietal cortex, this abrupt change in the timetable of histogenesis of primate areas 17 and 18 occurs between areas and contrasts with laminar histogenesis within each area, which remains largely constant. These findings in primates and rodents suggest that transient and steep changes in neurogenic gradients can lead to areal specific differences in the timetable of laminar histogenesis. However, Bayer and Altman (1991) report apparent reversals in neurogenic gradients. Such reversals might be required to maintain a constant timetable of laminar histogenesis within individual areas. However, one consequence of these reversals is the possibility of areal differences that are not consistent with the main rostrocaudal and lateromedial gradients.

Developmental significance and functional consequence of areal differences in laminar histogenesis

Changes in the timetable of layer histogenesis means that individual areas can devote varying amounts of neuron production to a given layer, which, along with cell death (Finlay and Slattery, 1983; Blaschke et al., 1996), could have important consequences for laminar neuron number in the adult. The present findings show that these areal differences can be generated during the production of infragranular and granular layers and before the arrival of ascending projections to the cortex. This result shows that this potentially important control mechanism of neuron number corresponds to an intrinsic regionalisation of laminar histogenesis.

CONCLUSION

The present findings show that there are important areal differences in the timing of generation of individual layers in isocortex and this may be a common feature of mammalian cortex. A major factor governing the timing of individual layer formation is the recruitment of precursors to the production of a particular layer. In this way, areal differences in laminar generation rate would be expected largely to reflect differences in the environmental signalling that commit precursors in their last cell cycle to a particular cortical layer (McConnell, 1988; McConnell and Kaznowski, 1991; Frantz and McConnell, 1996). Once precursors are committed to the generation of a particular cortical layer, modulation of the kinetics of the cell-cycle could make an important contribution to both the rate of formation and the dimensions of the cortical layer.

The present results demonstrate areal differences in laminar formation in the mouse isocortex and show that laminar specification is an integral part of areal specification. Furthermore, areal differences are found from E13.5 onward and therefore exist before the arrival of thalamic afferents in the vicinity of the cortex at E15.5 (Bicknese et al., 1994; Cohen-Tannoudji et al., 1994; Molnar and Blakemore, 1995; Polleux et al., 1996). These results, showing an early regionalisation of the ventricular zone, are in agreement with an increasing body of experimental results providing evidence of an early fate map of cortical areas at the level of the ventricular zone (Rakic, 1988; Barbe and Levitt, 1991; Arimatsu et al., 1992; Dehay et al., 1993; Kennedy and Dehay, 1993; Cohen-Tannoudji et al., 1994; Ebrahimi-Gaillard et al., 1994; Dehay et al., 1996; Ebrahimi-Gaillard and Roger, 1996).

ACKNOWLEDGEMENTS

The authors thank Christel Merrouche and Pascale Giroud for their excellent technical assistance. We also thank Dr. I.H.M. Smart for his constant reminder of the importance of neurogenic gradients in corticogenesis.

LITERATURE CITED

Angevine, J.B. (1965) Time of neuron origin in the hippocampal region. An autoradiographic study in the mouse. Exp. Neurol. *Suppl. 2:*1–70.

Angevine, J.B., and R.L. Sidman (1961) Autoradiographic study of cell migration during histogenesis of cerebral cortex in the mouse. Nature (Lond.) *192:*766–768.

Appleton, T.C., S.R. Pelc, and M.H. Tarbit (1969) Formation and loss of DNA in intestinal epithelium. J. Cell Sci. *5:*45–55.

Arimatsu, Y., M. Miyamoto, I. Nihonmatsu, K. Hirata, Y. Uratani, Y. Hatanaka, and K. Takigushi-Hayashi (1992) Early regional specification for a molecular neuronal phenotype in the rat neocortex. Proc. Natl. Acad. Sci. USA *89:*8879–8883.

Austin, C.P., and C.L. Cepko (1990) Cellular migration patterns in the developing mouse cerebral cortex. Development *110:*713–732.

Barbe, M.F., and P. Levitt (1991) The early commitment of fetal neurons to the limbic cortex. J. Neurosci. *11:*519–533.

Bayer, S.A., and J. Altman (1991) Neocortical Development. New York: Raven Press.

Beaulieu, C. (1993) Numerical data on neocortical neurons in adult rat, with special reference to the GABA population. Brain Res. *609:*284–292.

Berry, M., and A.W. Rogers (1965) The migration of neuroblasts in the developing cerebral cortex. J. Anat. *99:*691–709.

Bicknese, A.R., A.M. Sheppard, D.D.M. O'Leary, and A.L. Pearlman (1994) Thalamocortical axons extend along a chondroitin sulfate proteoglycan-enriched pathway coincident with neocortical subplate and distinct from the efferent path. J. Neurosci. *14:*3500–3510.

Bisconte, J.C., and R. Marty (1975) Étude quantitative du marquage radioautographique dans le système nerveux du rat. II. Caractéristiques finales dans le cerveau de l'animal adulte: Lois d'interprétation et concept de chronoarchitectonie corticale. Exp. Brain Res. *22:*37–56.

Blaschke, A.J., K. Staley, and J. Chun (1996) Widespread programmed cell death in proliferative and postmitotic regions of the fetal cerebral cortex. Development *122:*1165–1174.

Brückner, G., V. Mares, and D. Biesold (1976) Neurogenesis in the visual system of the rat: An autoradiographic investigation. J. Comp. Neurol. *166:*245–256.

Caviness, V.S. (1975) Architectonic map of the neocortex of the normal mouse. J. Comp. Neurol. *164:*247–264.

Caviness, V.S. (1976) Patterns of cell and fiber distribution in the neocortex of the reeler mutant mouse. J. Comp. Neurol. *170:*435–448.

Caviness, V.S. (1982) Neocortical histogenesis in the normal and reeler mice: A developmental study based upon [^{3}H]-thymidine autoradiography. Dev. Brain Res. *4:*293–302.

Caviness, V.S., and R.L. Sidman (1973) Time of origin of corresponding cell classes in the cerebral cortex of normal and reeler mice: An autoradiographic analysis. J. Comp. Neurol. *148:*141–152.

Caviness, V.S., T. Takahashi, and R.S. Nowakowski (1995) Numbers, time and neocortical neuronogenesis: A general developmental and evolutionary model. Trends Neurosci. *18:*379–383.

Cohen-Tannoudji, M., C. Babinet, and M. Wassef (1994) Early determination of a mouse somatosensory cortex marker. Nature *368:*460–463.

Cooper, J.D., J.N. Payne, and R.W. Horobin (1988) Accurate counting in frozen sections: Some necessary precautions. J. Anat. *157:*13–21.

Dehay, C., P. Giroud, M. Berland, I. Smart, and H. Kennedy (1993) Modulation of the cell cycle contributes to the parcellation of the primate visual cortex. Nature *366:*464–466.

Dehay, C., P. Giroud, M. Berland, H. Killackey, and H. Kennedy (1996) Contribution of thalamic input to the specification of cytoarchitectonic cortical fields in the primate: Effects of bilateral enucleation in the fetal monkey on the boundaries, dimensions, and gyrification of striate and extrastriate cortex. J. Comp. Neurol. *367:*70–89.

Dräger, U.C. (1981) Observations of the organisation of the visual cortex in the reeler mouse. J. Comp. Neurol. *201:*555–570.

Ebrahimi-Gaillard, A., and M. Roger (1996) Development of spinal cord projections from neocortical transplants heterotopically placed in the neocortex of newborn hosts is highly dependent on the embryonic locus of origin of the graft. J. Comp. Neurol. *365:*129–140.

Ebrahimi-Gaillard, A., J. Guitet, C. Garnier, and M. Roger (1994) Topographic distribution of efferent fibers originating from homotopic or heterotopic transplants: Heterotopically transplanted neurons retain some of the developmental characteristics corresponding to their site of origin. Dev. Brain Res. *77:*271–283.

Fernandez, V., and H. Bravo (1974) Autoradiographic study of the development of the cerebral cortex in the rabbit. Brain Behav. Evol. *9:*317–332.

Ferrer, I., E. Bernet, E. Soriano, T. Del Rio, and M. Fonseca (1990) Naturally occurring cell death in the cerebral cortex of the rat and removal of dead cells by transitory phagocytes. Neuroscience *39:*451–458.

Ferrer, I., A. Tortosa, R. Blanco, F. Martin, T. Serrano, A. Planas, and A. Macaya (1994) Naturally occurring cell death in the developing cerebral cortex of the rat: Evidence of apoptosis-associated internucleosomal DNA fragmentation. Neurosci. Lett. *182:*77–79.

Finlay, B.L., and M. Slattery (1983) Local differences in amount of early cell death in neocortex predict adult local specializations. Science *219:*1349–1351.

Frantz, G.D., and S.K. McConnell (1996) Restriction of late cerebral cortical progenitors to an upper-layer fate. Neuron *17:*55–61.

Fujita, S. (1963) The matrix cell and cytogenesis in the developing central nervous system. J. Comp. Neurol. *120:*37–42.

Gardette, R., M. Courtois, and J.-C. Bisconte (1982) Prenatal development of mouse central nervous structures: time of neuron origin and gradients of neuronal production: A radioautographic study. J. Hirnforsch. *23:*415–431.

Gillies, K., and D.J. Price (1993) The fates of cells in the developing cerebral cortex of normal and methylazoxymethanol acetate-lesioned mice. Eur. J. Neurosci. *5:*73–84.

Hardy, H., L. Heimer, R. Switzer, and D. Watkins (1976) Simultaneous demonstration of horseradish peroxydase and acetylcholinesterase. Neurosci. Lett. *3:*1–5.

Heumann, D., and G. Leuba (1983) Neuronal death in the development and aging of the cerebral cortex of the mouse. Neuropathol. Appl. Neurobiol. *9:*297–311.

Hicks, S.P., and C.J. D'Amato (1968) Cell migration to the isocortex in the rat. Anat. Rec. *160:*619–634.

Hoffart, R.M., J.G. Johnston, L.A. Krushel, and D. van der Kooy (1995) The mouse mutation *reeler* causes increased adhesion within a subpopulation of early postmitotic cortical neurons. J. Neurosci. *15:*4838–4850.

Ignacio, M.P.D., E.J. Kimm, G.H. Kageyama, J. Yu, and R.T. Robertson (1995) Postnatal migration of neurons and formation of laminae in the rat cerebral cortex. Anat. Embryol. *191:*89–100.

Jackson, C.A., J. Peduzzi, and T.L. Hickey (1989) Visual cortex development in the ferret. I. Genesis and migration of visual cortical neurons. J. Neurosci. *9:*1242–1253.

Jensen, K.F., and J. Altman (1982) The contribution of the late-generated neurons to the callosal projection in the rat: A study with prenatal X-irradiation. J. Comp. Neurol. *209:*113–122.

Jensen, K.F., and H.P. Killackey (1984) Subcortical projections from ectopic neocortical neurons. Proc. Natl. Acad. Sci. USA *81:*964–968.

Kennedy, H., and C. Dehay (1993) Cortical specification of mice and men. Cereb. Cortex *3:*27–35.

Kornack, D.R., and P. Rakic (1995) Radial and horizontal deployment of clonally related cells in the primate neocortex: relationship to distinct mitotic lineages. Neuron *15:*311–321.

Krieg, W. (1946a) Connections of the cerebral cortex I. The albino rat. A. Topography of the cortical areas. J. Comp. Neurol. *84:*221–275.

Krieg, W. (1946b) Connections of the cerebral cortex I. The albino rat. B. Structure of the cortical areas. J. Comp. Neurol. *84:*277–323.

Lemmon, V., and A.L. Pearlman (1981) Does laminar position determine the receptive field properties of cortical neurons? A study of corticotectal cells in area 17 of the normal mouse and the reeler mutant. J. Neurosci. *1:*83–93.

Luskin, M.B., and C.J. Shatz (1985) Neurogenesis of the cat's primary visual cortex. J. Comp. Neurol. *242:*611–631.

Luskin, M.B., A.L. Pearlman, and J.R. Sanes (1988) Cell lineage in the cerebral cortex of the mouse studied in vivo and in vitro with a recombinant retrovirus. Neuron *1:*635–647.

Luskin, M.B., J.G. Parnavelas, and J.A. Barlfield (1993) Neurons, astrocytes and oligodendrocytes of the rat cerebral cortex originate from separate progenitor cells: An ultrastructural analysis of clonally related cells. J. Neurosci. *13:*1730–1750.

McConnell, S.K. (1988) Fates of visual cortical neurons in the ferret after isochronic and heterochronic transplantation. J. Neurosci. *8:*945–974.

McConnell, S.K. (1996) Constructing the cerebral cortex: neurogenesis and fate determination. Neuron *15:*761–768.

McConnell, S.K., and C.E. Kaznowski (1991) Cell cycle dependence of laminar determination in developing neocortex. Science *254:*282–285.

Miller, M.W. (1988) Development of projection and local circuit neurons in neocortex. In A. Peters, and E.G. Jones (eds): Cerebral Cortex, Vol. 7. New York, London: Plenum Press, pp. 133–175.

Miller, M.W. (1992) Circadian rhythm of cell proliferation in the telencephalic ventricular zone: Effect of in utero exposure to ethanol. Brain Res. *595:*17–24.

Mitrovic, N., and M. Schachner (1996) Transient expression of NADPH diaphorase activity in the mouse whisker to barrel field pathway. J. Neurocytol. *25:*429–437.

Molnar, Z., and C. Blakemore (1995) How do thalamic axons find their way to the cortex? Trends Neurosci. *18:*389–397.

Moore, R., and J. Price (1992) The distribution of clones of neurons in the rat somatosensory cortex. J. Neurocytol. *21:*737–743.

Mustari, M.J., R.D. Lund, and K. Graubard (1979) Histogenesis of the superior colliculus of the albino rat: A tritiated thymidine study. Brain Res. *164:*39–52.

Nowakowski, R.S., S.B. Lewin, and M.W. Miller (1989) Bromodeoxyuridine immunohistochemical determination of the lengths of the cell cycle and the DNA-synthetic phase for an anatomically defined population. J. Neurocytol. *18:*311–318.

O'Leary, D.D.M. (1989) Do cortical areas emerge from a protocortex ? Trends Neurosci. *12:*400–406.

O'Rourke, N.A., M.E. Dailey, S.J. Smith, and S.K. McConnell (1992) Diverse migratory pathways in the developing cerebral cortex. Science *258:*299–302.

O'Rourke, N.A., D.P. Sullivan, C.E. Kaznowski, A.A. Jacobs, and S.K. McConnell (1995) Tangential migration of neurons in the developing cerebral cortex. Development *121:*2165–2176.

Parnavelas, J.G., J.A. Barfield, E. Franke, and M.B. Luskin (1991) Separate progenitor cells give rise to pyramidal and nonpyramidal neurons in the rat telencephalon. Cereb. Cortex *1:*463–468.

Pinto Lord, M.C., P. Evrard, and V.S. Caviness (1982) Obstructed neuronal migration along radial glial fibers in the neocortex of the reeler mouse: A Golgi-EM analysis. Dev. Brain Res. *4:*379–393.

Polleux, F., C. Dehay, and H. Kennedy (1996) Gradients and timing of the arrival of thalamic axons in the mouse neocortex. Soc. Neurosci. Abstr. *22:*1012.

Price, J., and L. Thurlow (1988) Cell lineage in the rat cerebral cortex: A study using retroviral-mediated gene transfer. Development *104:*473–482.

Raedler, E., and A. Raedler (1978) Autoradiographic study of early neurogenesis in rat neocortex. Anat. Embryol. *154:*267–284.

Raedler, E., A. Raedler, and S. Feldhaus (1980) Dynamical aspects of neocortical histogenesis in the rat. Anat. Embryol. *158:*253–269.

Rakic, P. (1973) Kinetics of proliferation and latency between the final division and onset of differentiation of the cerebellar stellate and basket interneurons. J. Comp. Neurol. *147:*523–546.

Rakic, P. (1974) Neurons in Rhesus monkey visual cortex: Systematic relation between time of origin and eventual disposition. Science *183:*425–427.

Rakic, P. (1976) Differences in the time of origin and in eventual distribution of neurons in areas 17 and 18 of the visual cortex in rhesus monkey. Exp. Brain Res. (Suppl.) *1:*244–248.

Rakic, P. (1988) Specification of cerebral cortical areas. Science *241:*170–176.

Rakic, P. (1995) Radial versus tangential migration of neuronal clones in the developing neocortex. Proc. Natl. Acad. Sci. USA *92:*11323–11327.

Rakic, P., and R.S. Nowakowski (1981) The time and site of origin of neurons in the hippocampal region of the rhesus monkey. J. Comp. Neurol. *196:*99–128.

Reid, C.B., I. Liang, and C. Walsh (1995) Systematic widespread clonal organization in the cerebral cortex. Neuron *15:*299–310.

Reznikov, K. (1990) Cell proliferation and cytogenesis in the mouse hippocampus. Adv. Anat. Embryol. Cell Biol. *122:*1–83.

Reznikov, K., and D. van der Kooy (1995) Variability and partial synchrony of the cell cycle in the germinal zone of the early embryonic cerebral cortex. J. Comp. Neurol. *360:*536–554.

Robertson, R.T., A.A. Tijerina, and M.E. Gallivan (1985) Transient patterns of Acetylcholinesterase activity in visual cortex of the rat: Normal development and the effects of neonatal monocular enucleation. Dev. Brain Res. *21:*203–214.

Robertson, R.T., M.A. Hanes, and J. Yu (1988) Investigation of the origins of transient acetylcholinesterase activity in developing rat visual cortex. Dev. Brain Res. *41:*1–23.

Rockel, A.J., R.W. Hiorns, and T.P.S. Powell (1980) The basic uniformity in structure of the neocortex. Brain *103:*221–224.

Rogers, A.W. (1967) Techniques of autoradiography. Amsterdam: Elsevier.

Sanderson, K.J., and W.L. Weller (1990) Gradients of neurogenesis in possum neocortex. Dev. Brain Res. *55:*269–274.

Schmahl, W. (1983) Developmental gradient of cell cycle in the telencephalic roof of the fetal NMRI-mouse. Anat. Embryol. *167:*355–364.

Schultze, B., B. Nowak, and W. Maurer (1974) Cycle times of the neural epithelial cells of various types of neuron in the rat: An autoradiographic study. J. Comp. Neurol. *158:*207–218.

Shatz, C.J. (1992) Dividing up the neocortex. Science *258:*237–238.

Shimada, M., and J. Langman (1970) Cell proliferation, migration and differentiation in the cerebral cortex of the Golden Hamster. J. Comp. Neurol. *139:*227–244.

Sidman, R.L. (1970) Autoradiographic methods and principles for study of the nervous system with thymidine-H3. In W.J.H. Nauta, and S.O.E. Ebbesson (eds): Contemporary Research Methods in Neuroanatomy. Berlin, Heidelberg, New York: Springer, pp. 252–274.

Silva, L.R., M.J. Gutnick, and B.W. Connors (1991) Laminar distribution of neuronal membrane properties in neocortex of normal and reeler mouse. J. Neurophysiol. *66:*2034–2040.

Simmons, P.E., and A.L. Pearlman (1983) Receptive-field properties of transcallosal visual cortical neurons in the normal and reeler mouse. J. Neurophysiol. *50:*838–848.

Skoglund, T.S., R. Pascher, and C.-H. Berthold (1996) Heterogeneity in the columnar number of neurons in different neocortical areas in the rat. Neurosci. Lett. *208:*97–100.

Skoglund, T.S., R. Pascher, and C.-H. Berthold (1997) The existence of a layer IV in the rat motor cortex. Cereb. Cortex *7:*178–180.

Smart, I.H.M., and M. Smart (1977) The location of nuclei of different labelling intensities in autoradiographs of anterior forebrain of postnatal mice injected with [3H]thymidine on the eleventh and twelfth day post-conception. J. Anat. *123:*515–525.

Smart, I.H.M., and M. Smart (1982) Growth patterns in the lateral wall of the mouse telencephalon. I. Autoradiographic studies of the histogenesis of the isocortex and adjacent areas. J. Anat. *134:*273–298.

Soriano, E., J.A. Del Rio, and C. Auladell (1993) Characterization of the phenotype and birthdates of pyknotic dead cells in the nervous system by a combination of DNA staining and immunohistochemistry for 5'-Bromodeoxyuridine and neural antigens. J. Histochem. Cytochem. *41:*819–827.

Soriano, E., N. Dumesnil, C. Auladell, M. Cohen-Tannoudji, and C. Sotelo (1995) Molecular heterogeneity of progenitors and radial migration in the developing cerebral cortex revealed by transgene expression. Proc. Natl. Acad. Sci. USA *92:*11676–11680.

Spreafico, R., C. Frassoni, P. Arcelli, M. Selvaggio, and S. De Biasi (1995) In situ labeling of apoptotic cell death in the cerebral cortex and thalamus of rats during development. J. Comp. Neurol. *363:*281–295.

Takahashi, T., R.S. Nowakowski, and V.S. Caviness (1995) The cell cycle of the pseudostratified ventricular epithelium of the embryonic cerebral wall. J. Neurosci. *15:*6046–6057.

Tan, S.-S., and S. Breen (1993) Radial mosaicism and tangential cell dispersion both contribute to mouse neocortical development. Nature *362:*638–639.

Tan, S.-S., B. Faulkner-Jones, S.J. Breen, M. Walsh, J.F. Bertram, and B.E. Reese (1995) Cell dispersion patterns in different cortical regions studied with an X-inactivated transgenic marker. Development *121:* 1029–1039.

Terashima, T., K. Inoue, Y. Inoue, K. Mikoshiba, and Y. Tsukuda (1983) Distribution and morphology of corticospinal tract neurons in reeler mouse cortex by the retrograde HRP method. J. Comp. Neurol. *218:*314–326.

Terashima, T., K. Inoue, Y. Inoue, K. Mikoshiba, and Y. Tsukuda (1985) Distribution and morphology of callosal commisural neurons within the motor cortex of normal and reeler mice. J. Comp. Neurol. *232:*83–98.

Valverde, F., L. Lopez-Mascaraque, M. Santanaca, and J.A. DeCarlos (1995) Persistence of early-generated neurons in the rodent subplate: Assessment of cell death in neocortex during the early postnatal period. J. Neurosci. *15:*5014–5024.

Vincent, S.R., and H. Kimura (1992) Histochemical mapping of nitric oxide synthase in the rat brain. Neuroscience *46:*755–784.

Waechter, R.V., and B. Jaensch (1972) Generation time of the matrix cells during embryonic brain development: an autoradiographic study in rats. Brain Res. *46:*235–250.

Walsh, C., and C.L. Cepko (1992) Widespread dispersion of neuronal clones across functional regions of the cerebral cortex. Science *255:*434–440.

Woo, T.U., and B.L. Finlay (1996) Cortical target depletion and ingrowth of geniculocortical axons: implications for cortical specification. Cereb. Cortex *6:*457–469.

Woolsey, T.A., and H. van der Loos (1970) The structural organization of layer IV in the somatosensory region (SI) of mouse cerebral cortex. Brain Res. *17:*205–242.